Master thesis

A dual polyphenolic/zwitterionic coating for prevention of microbial biofilm formation on urinary catheters

Andreas Ortner
Matriculation number: 0030608

zur Erlangung des akademischen Grades eines

Diplom-Ingenieurs

der Studienrichtung Biotechnologie

eingereicht an der

Technischen Universität Graz

November 2012

Supervisors: Dr. Carlos Díaz Blanco

Prof. Dr. TzankoTzanov

Prof. DI Dr. Georg Gübitz

„Die letzte Stimme, die man hört, bevor die Welt explodiert, wird die Stimme eines Experten sein, der sagt: 'Das ist technisch unmöglich!'“

Peter Alexander Ustinov

Abstract

Biofilms are bacterial communities encased in a self-produced hydrated polymeric matrix. Such level of organization provides the bacterial community with a high resistance to the immune system and to antibiotics, thus making them a common cause of implant-associated infections. Among the latter, urinary tract infections associated to the formation of biofilms on catheters account for approximately 40 % of all hospital-acquired infections.

In this master thesis, natural polyphenols from renewable resources with known antimicrobial activity against pathogenic bacteria were grafted onto pre-aminated silicone urinary catheters. In a second step, the polyphenolic coating was enzymatically activated by laccases through the formation of radical species and further modified by the introduction of zwitterionic moieties, known for their active role in the prevention of biofilm formation. The successful modification of the catheters was evaluated by means of chemical, physical and spectroscopic techniques while the efficiency of such enzymatically generated coatings against biofilm formation was assessed in static biofilm test showing significantly reduced microbial colonization of the silicone.

Kurzfassung

Biofilme sind bakterielle Gemeinschaften eingehüllt in einer selbst produzierten hydratisierten polymeren Matrix. Solche bakterielle Gemeinschaften zeigen eine hohe Widerstandsfähigkeit gegen das Immunsystems, sowie auch gegen Antibiotika, wodurch sie eine häufige Ursache von Implantat- assoziierten Infektionen darstellen. Rund 40% aller im Krankenhaus erworbenen Infektionen, die durch Bildung von Biofilmen auf Kathetern hervorgerufen werden, sind Harnwegsinfektionen.

In dieser Masterarbeit wurden natürliche Polyphenole aus nachwachsenden Rohstoffen mit bekannter antimikrobieller Aktivität gegen pathogene Bakterien auf preaminierte Silikon-Blasenkatheter aufgebracht. In einem zweiten Schritt wurde die polyphenolische Beschichtung enzymatisch durch Laccasen durch Radikalbildung aktiviert und durch die Zuführung von zwitterionischen Molekülen, die für die Verhinderung der Biofilmbildung bekannt sind, modifiziert. Die erfolgreiche Modifikation des Silikons wurde durch chemische, physikalische und spektroskopische Methoden bewiesen. Die Funktionalität dieser enzymatisch erzeugten Beschichtungen gegen Biofilmbildung wurde in statischen Biofilmtests eindeutig gezeigt.

STATUTORY DECLARATION

I declare that I have authored this thesis independently, that I have not used other than the declared sources / resources, and that I have explicitly marked all material which has been quoted either literally or by content from the used sources.

…… ……..

date (signature)

Danksagung

Ich möchte mich herzlich bei allen bedanken, die mir helfend unter die Arme gegriffen haben, sei es menschlich, seelisch, finanziell oder arbeitstechnisch. Dabei danke ich meiner Mutter, meinen Geschwistern, wie auch meinem Vater.

Einen besonderen Dank möchte ich noch meiner Freundin Caroline aussprechen, die mir immer sehr geholfen hat.

Weiters bin ich meinem Betreuer Dr. Carlos Díaz Blanco großem Dank verpflichtet, der mir mit seinem Wissen, wie auch mit Rat und Tat zur Seite stand und mich stets unterstützte.

Auch Prof Dr. Dipl.Ing. Georg Gübitz und Prof. Dr. Dipl.Ing. TzankoTzanov sei gedankt, die mir die Möglichkeit gegeben haben, in Spanien (Terrassa) meine praktische Arbeit zu machen.

Margarida, Toni, Guillem, Kamelia, Sonia, Teresa, Mari, Merce, Diana, Eva, Sundar und allen anderen Kollegen sei gedankt für die freundliche Unterstützung während der Arbeit.

Ein Dankeschön an alle meine Freunde und Bekannte, die mich menschlich vorangetrieben haben!

DANKE!!

Abbreviations

APTES	Amino-propyl-tri-ethoxy-silane
ABTS	2,2´-Azino-bis(3-ethylbenzothiazoline-6-sulfonic acid)
AHL	Acyl-homoserine lactones
BCA	bicinchoninic acid
BSA	bovine serum albumin
DMAPS	Dimethyl-ammonium-propane-sulfonate
DPPH	2,2-diphenyl-1-picrylhydrazyl
EC	commission number
EPS	extracellular polymeric substances
FITC	fluorescein isothiocyanate
FTIR	Fourier transform infrared spectroscopy
GA	gallic acid
h	hour
M	molar
mM	millimolar
mg	milligram
min	minute
ml	milliliter
nm	nanometer
OD	optical density
PEG	poly-ethylene-glycol
rpm	rounds per minute
s	second
t-BHP	*tert*-Butylhydroperoxide
U	unit
UV	ultra violet
µg	microgram
XPS	X-ray photoelektron spectroscopy

Content

1. Introduction

Urinary tract infections, surgical site infections, respiratory tract infections and bloodstream infections are the four most common causes of hospital acquired infections. The most frequently reported nosocomial infections are urinary tract infections which are up to approximately 40% of all these infections. Most of them are associated with urinary catheters. Indwelling urinary catheters are used in 15–25 % of short-term care patients during their hospitalization and confer a predisposition to bacteriuria. 1–5 % of catheter-associated bacteriuria episodes cause secondary blood stream infections, which can be a serious risk with life-threatening complications [1] [2].

Urinary catheters allow bacterial colonization which leads to the biofilm formation on their inner and outer surfaces and hence to infections, which are difficult to eradicate by antibiotics. *Staphylococcus aureus* and *Staphylococcus epidermidis*are the most common bacteria involved in catheter related infections. Some organisms on the urinary catheter biofilm, such as *Proteus spp.*, *Pseudomonas aeruginosa*, *Klebsiella pneumoniae*, and *Providencia spp*. are able to synthesize the enzyme urease. This enzyme gives them the opportunity to hydrolyze urea in the urine to free ammonia. The ionic components in the urine then start to precipitate due to the alkaline environment. This ongoing progress of encrustation coupled with biofilm formation can completely block the catheter flow [1] [3] [4].

Prevention of urinary catheter biofilm formation has important implications in the treatment of urinary tract infections in catheterized patients. The colonized catheter must be replaced frequently which results in an increased morbidity and increasing costs to the healthcare system. Thus, the need to develop catheters with materials that prevent the attachment of microorganisms and the formation of biofilms is of paramount importance. Literature describes various modifications with hydrophilic outer layers, antimicrobial coated surfaces, low surface energy materials, highly biocompatible substances, biodegradable materials, and cell or protein grafted surfaces that showed good capability against microbial colonization. A plenty of papers demonstrated that the coating of biomaterials surfaces with heparin [5],

chitosan [6], a combination of heparin and chitosan [7], cationic charge [8], mucin [9] or cranberry-derived proanthocyanidins [10] substantially reduced the adhesion and colonization of bacteria. Since heparin has also antithrombogenic properties, it was also used for the surface modification of biomaterials through either chemical binding or physical absorption [11]. Impregnation with antimicrobials on catheters was also reported: Antimicrobial agents such as furanones [12], silver oxide [13], antibiotics like ciprofloxacin, ofloxacin, norfloxacin [14] [15], a combination of antibiotics (minocycline with rifampicin) [16], titanium dioxide [17] or a combination of silver oxide with titanium dioxide [18] showed promising results for biofilm reduction/inhibition on urinary catheters or potential urological biomaterials.

The aim of this work was to create an antibiofim/antifouling surface of a urinary catheter. First the silicone is getting silanized with APTES to provide a functional group on the surface. Then the enzyme laccase is used in two steps: phenolic grafting of gallic acid which is known as a biocide and subsequent grafting of DMAPS on them to benefit of the zwitterionic moieties of the chemical compound.

2. Theoretical background

2.1 Biofouling

The accumulation of microorganisms, plants, algae, or animals on wet surfaces is called biofouling. If the host surface is another organism, such accumulation is referred to as epibiosis, a relationship which is not parasitic.

The diversity among biofouling organisms is very high and extends far beyond attachment of sea shells and seaweeds. Ship hulls for example become fouled with marine organism after a very short time, wherefore more than 4000 species can be responsible [19]. Biofouling can be divided into two areas: 1. Microfouling: biofilm formation and bacterial adhesion and 2. Macrofouling: attachment of larger organisms. There is also a classification for hard or soft fouling types. Mussels, barnacles, encrusting bryozoans, mollusks, polychaete and other tube worms are included in the calcareous (hard) fouling organisms. Seaweed, hydroids, algae and biofilm "slime" are examples of non-calcareous soft fouling organisms [20]. The hulls of marine vessels are good examples of surfaces prone to biofouling. They often become coated with marine organisms and their secretions, decreasing the efficiency of propulsion and contributing to higher fuel consumption [21].

In the medical environment, the biofouling problem refers more to components of biofluids such as proteins, cells and pathogens. These components have a propensity to strongly adhere to surfaces and alter their performance with potentially hazardous outcomes. Microbial colonization of catheters is causing urinary tract infections, which represents the most common hospital acquired infection [22]. Also microbial influenced corrosion in implanted medical devices is leading to the need for replacement surgeries with increased risk of infection [23].

2.2 Biofilms

A biofilm is an accumulation of microorganisms in which cells adhere to each other on living or non-living surfaces. These agglutinated cells are frequently embedded within a self-produced polymeric matrix which is a conglomeration composed of extracellular DNA, proteins and polysaccharides [24] [25], mainly called extracellular polymeric substances (EPS).

The biofilm formation starts with an attachment of free floating microorganisms or even proteins produced by microorganisms which can adhere to the surface initially through weak, reversible adhesion like van der Waals forces. After a short period of time, they start to form a transient association with the surface and/or other microbes previously attached to the surface (see figure 1).

During colonization the cells are able to communicate via quorum sensing using auto inducer signals, such as acyl-homoserine lactones (AHLs). Once colonization has started, the biofilm grows through a combination of cell division and recruitment. The final stage of biofilm formation is known as development where the biofilm is established and may only change in shape and size. If the biofilm is formed, it may allow for an aggregate cell colony (or colonies) to be increasingly resistant to antibiotics and other environmental threats. Bacteria growing in a biofilm can be up to 1000 times more resistant to antibiotics and less conspicuous to the immune system, because antigens are hidden and key ligands are suppressed [26].

It is becoming increasingly evident that biofilms are an enormous problem in medicine. Biofilms appear on many medical implants such as catheters, artificial hips and contact lenses. Because of their resistance to antimicrobial agents, these infections can often only be treated by removal of the implant, thus increasing the trauma to the patient and, in addition, the cost of the treatment. It has been estimated that biofilms are associated with 65 % of nosocomial infections [27] and the treatment of these biofilm-based infections costs more than $1 billion annually [28] [29] [30].

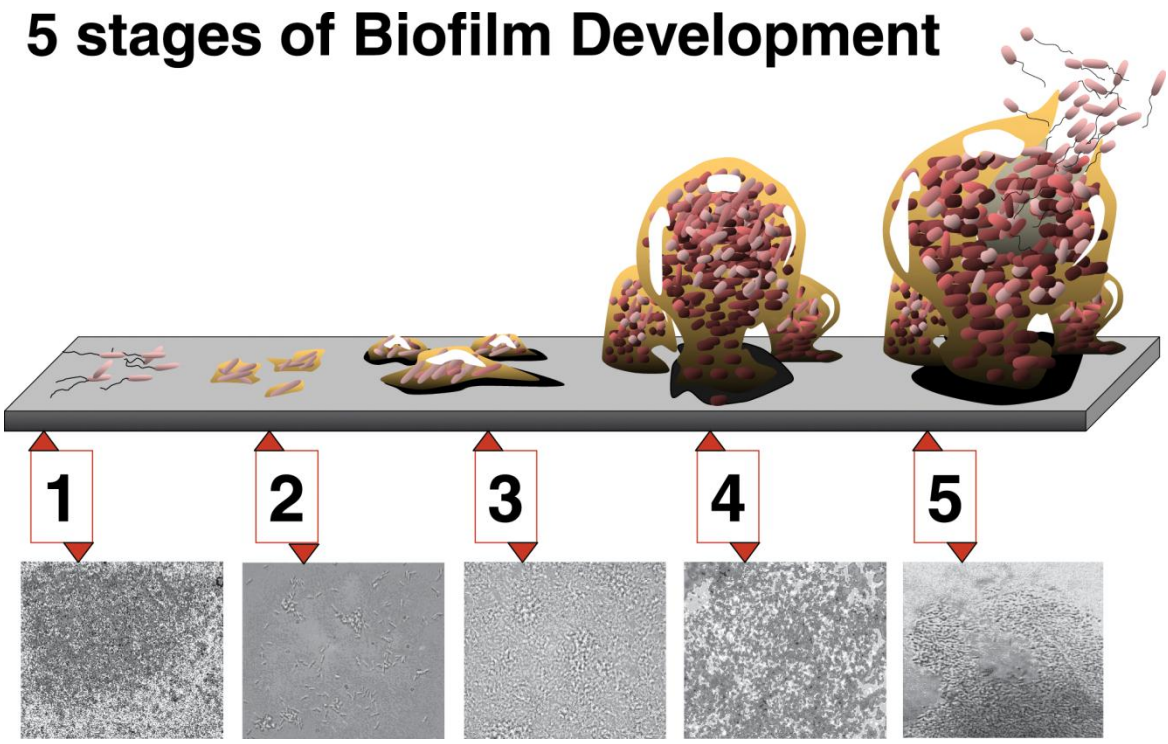

Figure 1: Stages of biofilm formation.
Stage 1: initial attachment; stage 2: irreversible attachment; stage 3: maturation I; stage 4: maturation II; stage 5: dispersion. Each stage of development in the diagram is paired with a photomicrograph of a developing *P. aeruginosa* biofilm. All photomicrographs are shown to same scale. Image credit: D. Davis [31]

2.3 Enzymes

Enzymes are proteins, which catalyze chemical reactions. In enzymatic reactions, the so called substrates are converted into different molecules, called products. Most of the spontaneous reactions in a biological cell would need longer than the lifetime of an animal to take place. That's why all chemical reactions in a biological cell need enzymes in order to occur at rates sufficient for life. Each enzyme speeds up only few reactions among many possibilities and therefore they are selective for their substrates. The set of enzymes produced in a cell determines which metabolic pathways occur in that cell.

Enzymes are lowering the activation energy for a reaction and hence increasing the rate of the reaction dramatically. As a result, reactions reach their equilibrium state faster and also the product output is more rapid. Another advantage is that enzymes are not consumed by the reactions they catalyze, nor do they alter the equilibrium of these reactions. Enzymes, in comparison with most other catalysts, are highly specific for their substrates. According to the BRENDA database there are now more than 5700 enzymes known which catalyze biochemical reactions.

Enzyme activity can also be influenced by other molecules like inhibitors and activators, which are molecules that decrease (for example: poison and drugs) or increase the enzyme activity respectively. Other properties that can have an influence on the enzyme activity are temperature, pressure, chemical environment e.g. pH, and also the concentration of the substrate.

Most enzymes are much bigger than the substrates they act on and only around 2–4 amino acids of the enzyme are directly involved in catalysis. The region that contains these catalytic residues is known as the active center. This active center interacts with the substrate and the reaction occurs. Some enzymes also have binding sites for cofactors (organic or inorganic non-protein molecules like flavin or cobalt) which are needed for catalysis.

Enzyme classes:

All Enzymes have a commission number (EC number) and are classified in 6 main categories according to the distinct reactions they catalyze (see table 1).

Table 1: Enzyme classification

EC #	Enzymatic class
EC1	Oxidoreductases
EC2	Transferases
EC3	Hydrolases
EC4	Lyases
EC5	Isomerases
EC6	Ligases

Depending on the exact chemical reaction catalyzed by an enzyme there also exist sub- and sub-sub-classes.

Kinetic:

The most common model used to describe enzyme kinetics is the Michaelis- Menten kinetic. The following simplification of an enzymatic reaction is the basis of the Michaelis- Menten equation, with the assumption, that the reaction P to ES is very slow:

$$E + S \underset{k_r}{\overset{k_f}{\rightleftharpoons}} ES \xrightarrow{k_{\text{cat}}} E + P$$

Formula 1: Enzyme catalyzed reaction.
S: substrate; E: enzyme; ES: enzyme-substrate complex; P: product; kf ,kr and kcat: velocity constant

If formula 1 is converted, all velocity constants can be combined into the so called Michaelis constant Km. Km is the substrate concentration, where the enzyme is working with half maximum velocity.

$$Km = (Kr + Kcat)/Kf$$

Formula 2: Km constant for Michaelis- Menten kinetics.

By further conversions, the Michaelis- Menten derived equation is obtained, which describes the reactions velocity V of an enzyme and the correlation with the Michaelis- Menten constant Km and the substrate concentration [32]:

$$V = Vmax * \frac{[S]}{Km + [S]}$$

Formula 3: Michaelis- Menten equation.
V: enzyme velocity; Vmax: maximum enzyme velocity; [S] substrate concentration; Km: Michaelis-Menten constant.

In the last few years enzymes showed more and more importance in almost all technological areas. The growing research in molecular and environmental biotechnology launches many types of new enzymes. This makes the enzymes cheap enough for using them in several processes, especially those, where up to now chemicals were used.

2.3.1 Laccase

Laccases have emerged as important enzymes due to their advantage of being environmental-friendly. Laccases are eco-friendly, due to their use of air and production of water as their only by-product. Furthermore they work under mild and energy-saving conditions.

These are very important qualities in a conscientious society that is increasingly becoming eco and energy-sensitive.

Laccases are multicopper containing enzymes which belong to the class of oxidoreductases. The four copper ions are bounded in several sides: Type 1 copper confers the typical blue color on the enzyme due to intense electronic absorption of covalent copper‑cysteine bonds. It is involved in the mono electronic substrate oxidation; the Type 2 and two Type 3 copper ions are forming a tri-nuclear cluster [33], to which the electrons are transferred and molecular oxygen is reduced to water. So laccase oxidizes four molecules of suitable substrate and produces four radicals while reducing one molecule of oxygen to two molecules of water (figure 2). A number of non-enzymatic reactions which include covalent coupling to form dimers,

oligomers and polymers through C-C, C-O and C-N bonds [34][35], degradation of complex polymers by cleavage of covalent bonds especially alkyl-aryl-bonds (sometimes in the presence of mediators), releasing monomers [36] [37] and ring cleavage of aromatic compounds [38] [39] [40] can then be catalyzed by these radicals.

Laccases have a very broad substrate range and therefore the application areas for this enzyme are increasing. Essentially, laccase is able to oxidize any substrate with characteristics similar to a p-diphenol. There are also some high redox potential fungal laccases which can oxidize monophenols such as cresol while others are able to oxidize non-phenolic molecules such as ascorbic acid [41]. If there are other substrates of interest, which cannot be oxidized solely because of a particularly high redox potential or of steric hindrance, they can be oxidized by laccase-radicalised mediators [33]. Therefore, the number of different substrates increased including also non-phenolic molecules. The consequent research on laccase, also in different sources, is opening new opportunities for a number of industries, for example in the textile-, food-, pulp and paper-, cosmetic-, and pharmaceutical industry. Laccases can also be used in biosensors and for the organic synthesis [42] [43].

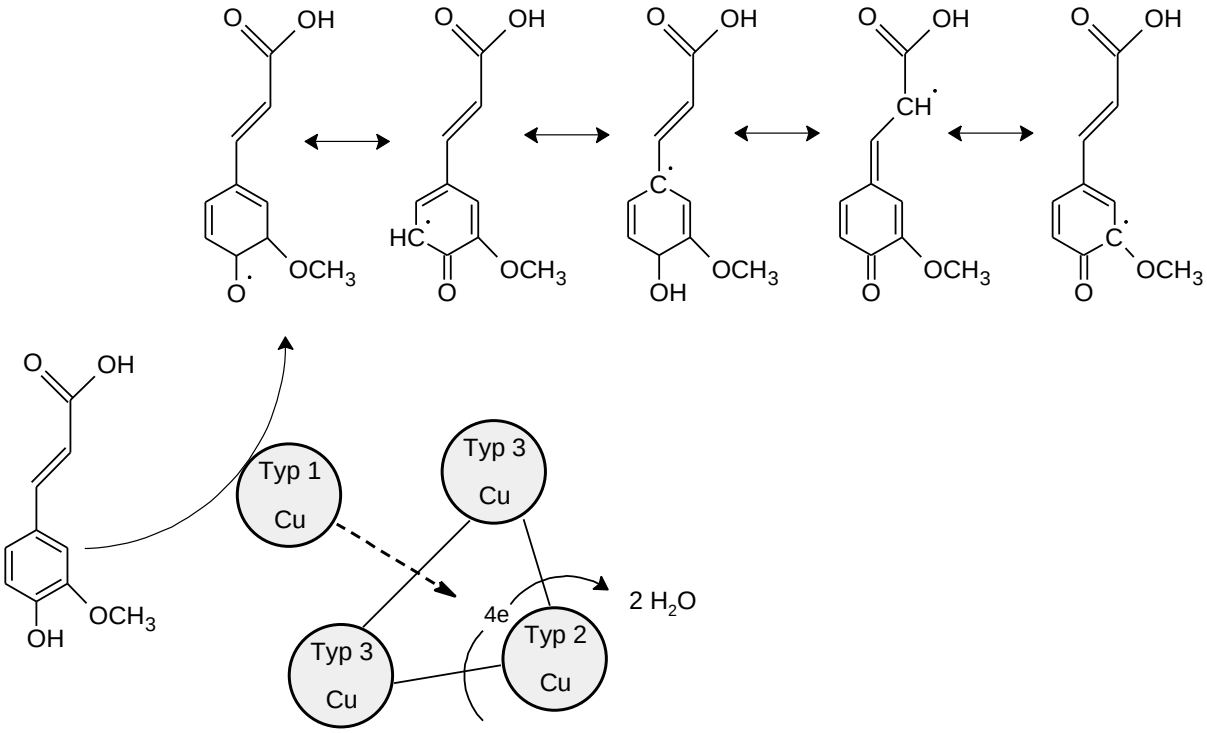

Figure 2: Laccase oxidation reaction of a suitable substrate, using coniferyl alcohol as an example [42]. Laccase has four different types of copper ions. Type 1 copper confers the typical blue color on the enzyme and is involved in the mono electronic substrate oxidation. The type 2 and two type 3 copper ions are forming a tri-nuclear cluster to which the electrons are transferred and molecular oxygen is reduced to water. So laccase oxidizes four molecules of suitable substrate and produces four radicals while reducing one molecule of oxygen to two molecules of water.

The following figures show the three dimensional structure of a bacterial-, fungi-, and plant- laccase. Laccases have 3 sequentially arranged cupredoxin-like domains at their 3-D structure level. Compared to plant and fungi, bacterial laccases have a larger binding cavity. The basis for their diverse functions is the difference in the residues of the copper binding site.

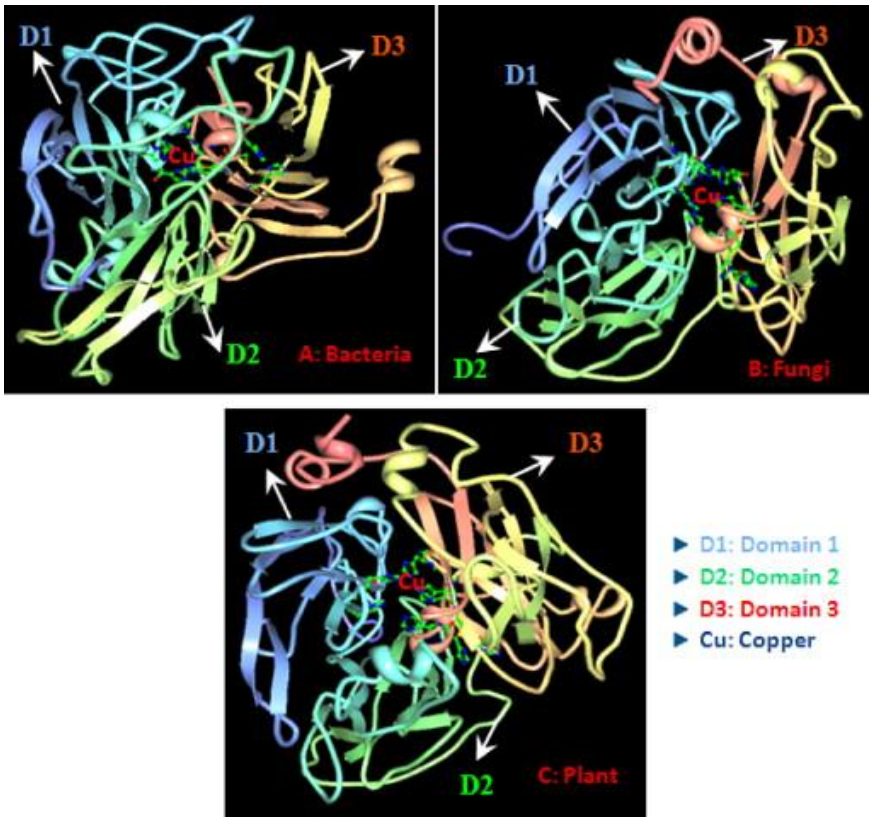

Figure 3: Three dimensional structure of laccase from bacteria, fungi and plant.
(A) bacterial laccase (*Bacillus subtilis*), (B) fungi laccase (*Tramates versicolor*), and (C) plant laccase (*Populus trichocarpa*) [44].

2.3.1.1 Laccase DENILITE IIS

DENILITE IIS is a special laccase mediator (methyl syringate) system. It has a clogged small molecule (mediator) which can enhance or widen the enzymes substrate specificity, so even big substrate molecules like lignin can be degraded (see figure 4).

Some fungi, like the white-rot fungi, are able to degrade lignin using a cocktail of oxidative enzymes, including laccases, despite the fact that the bulkiness of this polymer prevents direct interaction with these enzymes. Indeed, some scientists reported that the treatment of pulp with laccase alone does not catalyze the degradation of lignin but instead leads only to minimal structural changes and re-polymerization [45]. So it has been hypothesized that small molecules might act as red-ox shuttles between the enzyme's active site and the lignin core and cause polymer degradation [46].

So far, the effect of chemical mediators on laccase-catalyzed reactions has been evaluated extensively. The first artificial mediator used in the laccase-mediator system for pulp delignification was ABTS (2,2´-Azino-bis(3-ethylbenzothiazoline-6-sulfonic acid)) which was published in 1990 [46].

a.

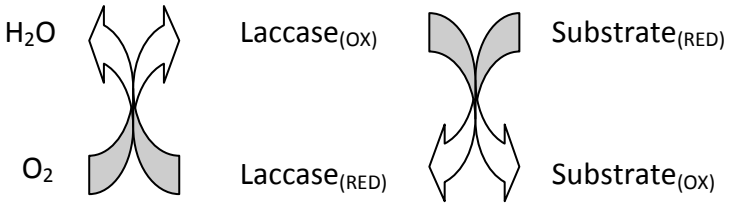

b.

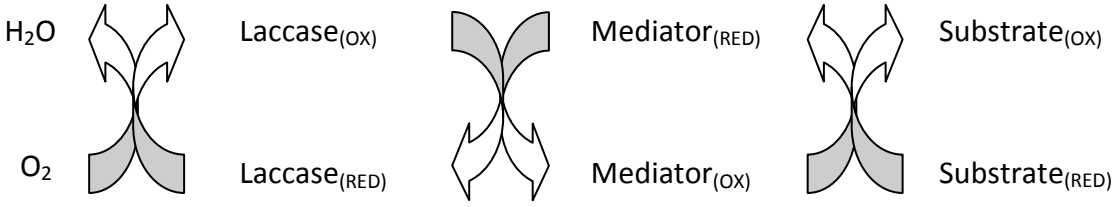

Figure 4: Schematic representation of laccase-catalyzed redox cycles for substrates oxidation. (a**) in the absence or (b) in the presence of chemical mediators**
DENILITE IIS is a special laccase mediator (methyl syringate) system. It has a clogged small molecule (mediator) which can enhance or widen the enzymes substrate specificity, so even big substrate molecules like lignin can be degraded.

2.4 Silanization reaction

The silanization reaction is a self-assembly condensation reaction between hydroxyl groups and chemical groups on the surface. Normally silanes have the chemical structure R_mSiX_n (where X is a hydrolysable group-often alkoxy groups and R an organic functionalized residue) which means, they can form silanol through hydrolysis with water ($R_mSi(OH)_n$). In a similar way they can react with OH or COOH groups on the surface and build a similar compound.

It is possible to provide a functionalized group on the silicones surface by using APTES (Amino-propyl-tri-ethoxy-silane), which is an alkoxysilane with a primary amino group as its organic function. The silanization reaction on silicone surfaces using APTES is shown in figure 5.

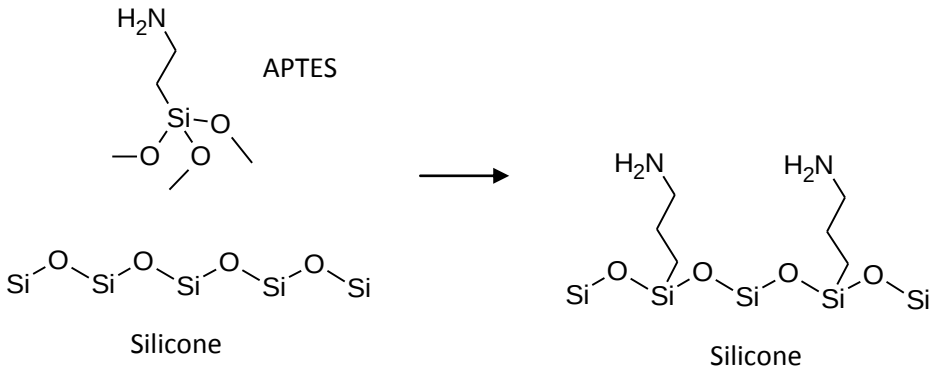

Figure 5: Silanization reaction on silicone surface with APTES.
Silanization reactions are used to provide functionalized groups on the surface for further utilizations. APTES is an alkoxysilane with a primary amino group as its organic function.

2.5 Laccase mediated phenol – amino coupling

2.5.1 Gallic acid

Gallic acid is a3,4,5-trihydroxybenzoic acid, which can be found in gallnuts, sumac, witch hazel, tea leaves, oak bark, and some other plants [48].Also a lot of different groceries contain gallic acid such as chocolate, mango, wine and vinegar. The chemical formula is $C_6H_2(OH)_3COOH$. Gallic acid can be found free and as part of tannins.

Commonly gallic acid is used in the pharmaceutical industry. The phenol content of various analysts is determined by the Folin-Ciocalteau assay where the gallic acid is used as a standard [49].

Gallic acid seems to have anti-fungal and anti-viral properties [50] and is described as a biocidal agent [51]. This phenolic acid is acting as an antioxidant and helps to protect human cells against oxidative damage. It was also found to show cytotoxicity against cancer cells [52], without harming healthy cells and it is used as a remote astringent in cases of internal hemorrhage [53]. Furthermore it can also be found in albuminuria and diabetes treatments [54], like in some ointments for the treatment of psoriasis and external hemorrhoids [55].

The gallic acid molecule is basically planar and the hydrogen atoms of the three hydroxyl groups which form intra- and intermolecular hydrogen bonds are oriented in the same direction around the ring. All available intermolecular hydrogen bonds are stabilizing the crystal structure [56]. Gallic acid is a strong chelating agent and forms highly stable complexes with iron. The chemical structure of gallic acid can be seen in figure 6.

The infrared spectrum of gallic acid shows a sharp absorption band of the carboxylic group -COOH at 1664 cm^{-1}, absorption bands of -OH at 1428 and at 864 cm^{-1}, as well as C-OH at 1320 cm^{-1} [57].

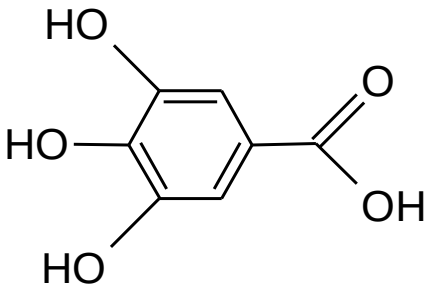

Figure 6: Chemical structure of gallic acid.

2.5.2 Phenol- amino coupling

This connection can proceed via Michael addition [58] or via radical coupling to get C–N bonds [59] as shown in figure 7. Although these experiments are based on radical coupling through the laccase, similar products can also be obtained through Michael addition.

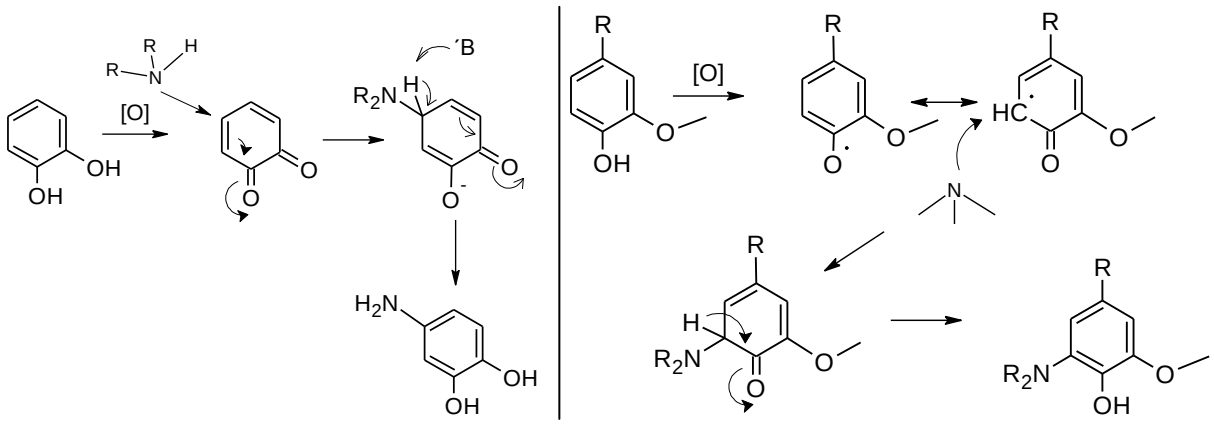

Figure 7: Laccase mediated phenol – amino coupling [60].
The phenol-amino coupling can be achieved via the Michael addition to a quinine (left side) and the radical coupling reaction to form a C-N bond (right side).

2.5.3 DPPH (2,2-diphenyl-1-picrylhydrazyl) test

DPPH is characterized as a stable free radical due to the delocalization of the spare electron over the molecule. Thus, the molecule cannot dimerize, as it would happen with other free radicals. The DPPH has a deep violet color in solution, characterized by an absorption band at about 520 nm. When a DPPH solution is mixed with a substance which can donate a hydrogen atom, for example an antioxidant like a phenol (figure 8), it generates the reduced form which is accompanied by the decrease of absorbance at 520 nm [61].

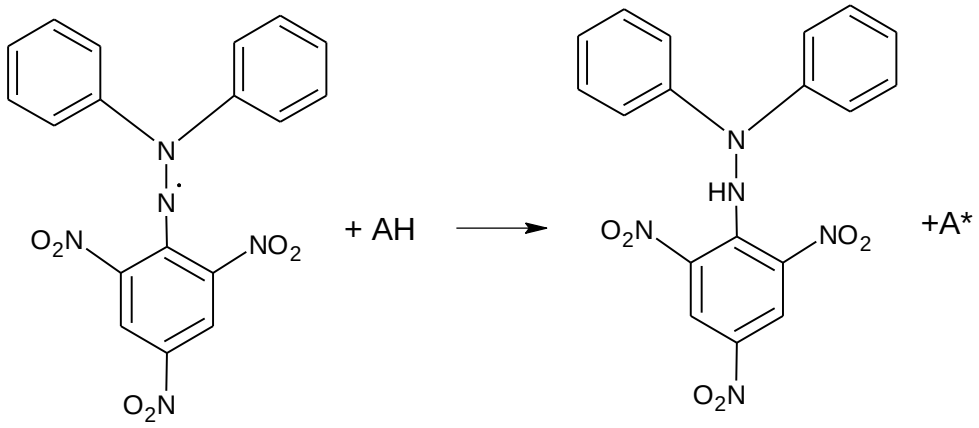

Figure 8: Reaction of a DPPH radical with an antioxidant.
DPPH is characterized as a stable free radical due to the delocalization of the spare electron over the molecule and has an adsorption band at about 520 nm. When a DPPH solution is mixed with an antioxidant like a phenol, or any other substance which can donate a hydrogen atom, it generates the reduced form which is accompanied by the decrease of absorbance at 520 nm.

2.6 Zwitterionic surface

An upcoming approach to prevent biofilms and incrustation is to create a nonfouling surface to prevent protein adsorption. In this context, the modification of surfaces with poly-ethylene-glycol (PEG) has been one of the most used methods [62] [63]. Recently, polymers of zwitterionic (positively and negatively charged) molecules like dimethyl-ammonium-propane-sulfonate (DMAPS) show high potential in improving nonfouling properties of surfaces and have been proven to prevent protein adsorption and cell adhesion [64] [65] [66] [67]. Creating a highly hydrophilic surface is considered to be the basic for the resistance of zwitterionic polymers to nonspecific protein adsorption. The capability of zwitterions to bind a significant number of water molecules gives them an excellent antifouling property. Furthermore, neutral charged material is another key factor for protein repulsion by reducing charge interactions with protein molecules.

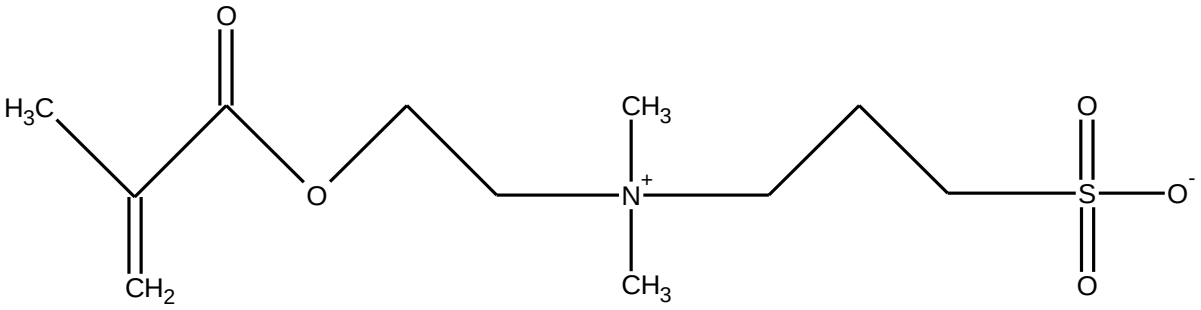

Figure 9: Chemical structure of Dimethyl-ammonium-propane-sulfonate (DMAPS).

2.7 FITC (fluorescein isothiocyanate)

FITC is a derivative of fluorescein and has many applications, for example in flow cytometry. The original fluorescein molecule is functionalized with an isothiocyanate reactive group (-N=C=S), which is replacing a hydrogen atom on the bottom ring of the structure (figure 10). FITC is reactive towards nucleophiles including amine and sulfhydryl groups on proteins.

This derivate has excitation and emission λ_{max} of approximately 495 nm and 521 nm respectively. Like most fluorochromes it is susceptible to photo bleaching.

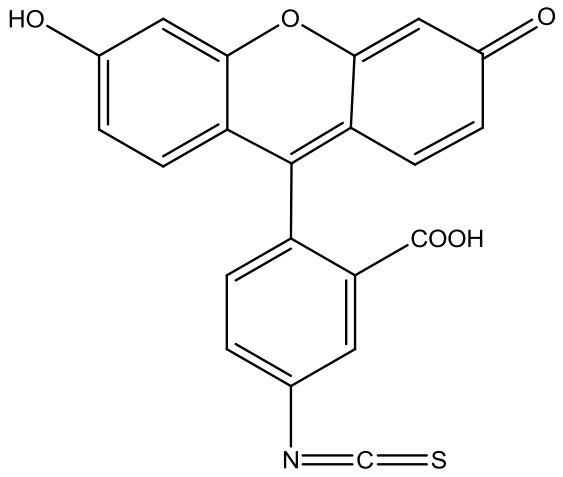

Figure 10: Chemical structure of fluorescein isothiocyanate.

2.8 Fourier transform infrared spectroscopy (FTIR)

FTIR is a technique which is used to get an infrared spectrum of absorption, emission, photoconductivity or Raman scattering of a solid, liquid or gaseous sample. An FTIR spectrometer simultaneously collects spectral data in a wide spectral range. “Fourier transform” is a mathematical process which is required to convert the big amount of data into the actual spectrum by a computer.

The goal of any absorption spectroscopy is to measure how a sample absorbs light at each different wavelength. Therefore it radiates a beam containing many frequencies of light at once, and measures how much of that beam is absorbed by the sample. The beam is generated by a broadband light source, which contains the full spectrum of wavelengths to be measured. The light goes through a configuration of mirrors, called Michelson interferometer (see figure 11) which allows to record an interferogram as the mirror is moving (due to wave interference). The interferogram is the mathematical equivalent of the spectrum and therefore a computer processing is required to convert the raw data (intensity of the interfering beam for each mirror position) into light absorption for each wavelength [68].

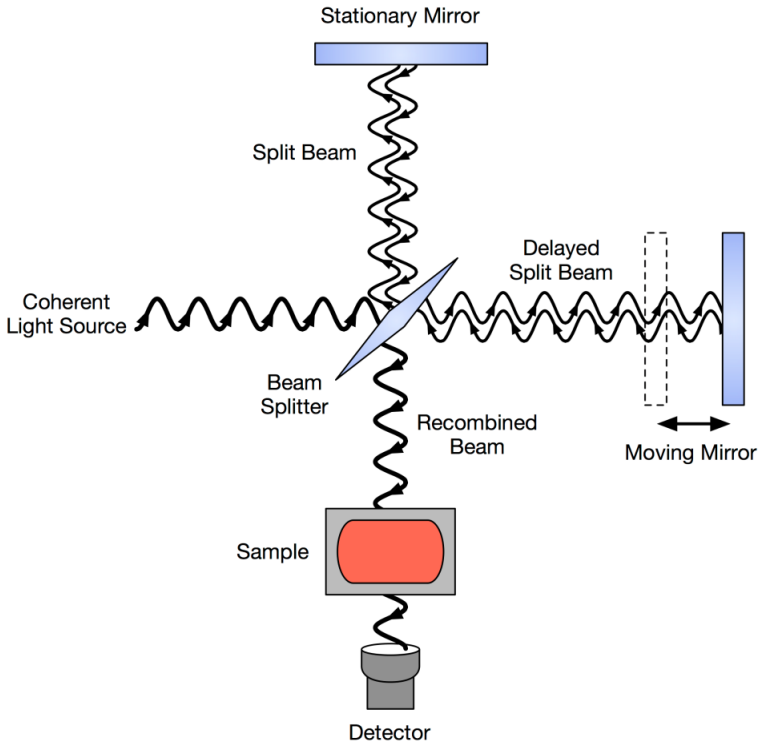

Figure 11: Schematic diagram of a Michelson interferometer, configured for FTIR.
The beam is generated by a broadband light source, which contains the full spectrum of wavelengths to be measured. The light goes through a configuration of mirrors, called Michelson interferometer, which allows to record an interferogram as the mirror is moving. Computer processing is required to convert the interferogram into light absorption for each wavelength.

2.9 X-ray photoelectron spectroscopy (XPS)

XPS is a quantitative spectroscopic technique that measures the elemental composition, empirical formula, chemical state and electronic state of the elements that exist in the top 1 to 10 nm of a sample. It starts by irradiating a material with a beam of X-rays while simultaneously measuring the kinetic energy and number of electrons that escape from the surface.

Normally a XPS spectrum is a spectrum of the number of electrons detected (sometimes per unit time) on the Y-axis (ordinate), versus the binding energy of the electrons detected on X-axis (abscissa). Each element that exist on the surface of the analyzed sample produces a specific set of XPS peaks at characteristic binding energy values that identify each element. These characteristic peaks correspond to the electron configuration of the atomic electrons (1s, 2s, 2p, 3s, etc.). All the detected electrons in each of the characteristic peaks can be directly related to the amount of element within the irradiated area. For the calculation of atomic percentage values, each raw XPS signal must be corrected by dividing the number of electrons detected by a "relative sensitivity factor" (RSF) and so normalize it over all of the elements detected.

All electrons at each kinetic energy value are captured by an electron counting detectors which is typically in a distance of one meter from the material irradiated with X-rays. Therefore the analysis must be performed under ultra-high vacuum conditions to minimize errors.

However, it is important to note that XPS detects only those electrons that have actually escaped into the vacuum of the instrument which appear normally from the top 10 to 12 nm of the material. In fact, X-rays are penetrating 1-5 µm of the sample but these deeper emitted electrons are either recaptured or trapped in various excited states within the material. For most applications XPS can be described as a non-destructive technique which displays the surface chemistry of any material.

The principle assembly of a XPS system can be seen in figure 12.

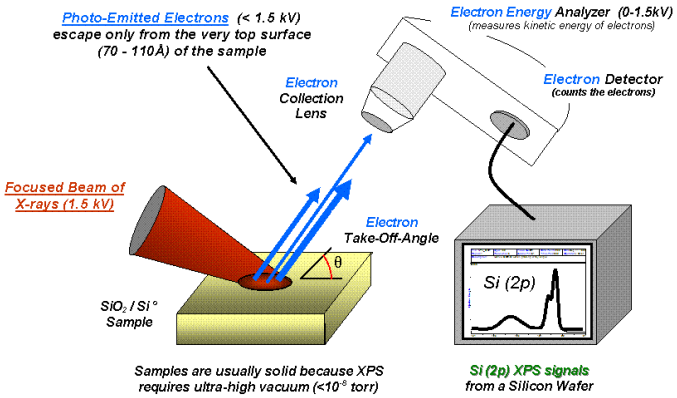

Figure 12: XPS analysis systems.
On the left side a vacuum chamber for XPS analysis, with hemispherical analyzer and X-ray tube (Foto: David Schrupp) and on the right side are the basic components of a monochromatic XPS system.

3. Material and methods

3.1 Chemicals

All used chemicals were of HPLC grade quality and purchased from Sigma Aldrich (Germany) or Scharlau (Spain). Deionized water was used.

Table 2: Used chemicals.

Chemicals	Supplier
Bicinchoninic Acid (BCA) Protein Assay Kit	Sigma-Aldrich
Sodium phosphate monobasid	Sigma-Aldrich
Sodiumchloride	Sigma-Aldrich
Sodium Potassium Tartrate, tetrahydrate	Sigma-Aldrich
Sodium hydroxide	Sigma-Aldrich
3,5-Dinitrosalicylic Acid	Sigma-Aldrich
3-aminopropyl-triethoxysilane	Sigma-Aldrich
Methanol abs.	Sigma-Aldrich
Sodium dodecyl sulfate	Sigma-Aldrich
Ninhydrin reagent, 2 % solution	Sigma-Aldrich
Fluorescein isothiocyanate	Sigma-Aldrich
Urea	Sigma-Aldrich
Disodium hydrogen orthophosphate	Sigma-Aldrich
Ammonium chloride	Sigma-Aldrich
Potassium dihydrogen orthophosphate	Sigma-Aldrich
Creatinine	Sigma-Aldrich
Sodium sulfite	Sigma-Aldrich
Ethanol 96 %	ScharlauScharlab
Dimethyl-ammonium-propane-sulfonate	Sigma-Aldrich
Succinic acid	Sigma-Aldrich
Bovine serum albumin	Sigma-Aldrich
Gallic acid	Sigma-Aldrich

3.2 Enzyme

The laccase DENILITE IIS (EC number 1.10.3.2) was purchased from Novozymes.

The DENILITE IIS laccase gene is from *Myceliophthora thermophila* expressed in *Aspergillus oryzae*. The structure of the *M. thermophila* laccase consists of a single peptide chain with three internal disulfide bonds and four copper atoms. The molecular mass of this laccase is 85 kDa.

3.2.1 Enzyme concentration

For calculating the protein concentration, a calibration with BCA – according to the instruction manual for the Bicinchoninic Acid Kit (SIGMA) – was performed and measured using a plate reader.

Therefore 8 mg of DENILITE Laccase powder was mixed in 1 ml sodium succinate buffer (pH 5) for 5 minutes and then centrifuged. The supernatant was used.

The amount of laccase (µg/mL) was determined using a platereader Infinite M200 from Tecan (Switzerland). The procedure was followed according to the instruction manual for the protein assay in 96-well culture plates [69].

3.2.2 Enzyme activity

3.2.2.1 Temperature profile

The enzymatic activity of the laccase was measured using the soluble substrate ABTS (2, 2′-azino-bis-(3-ethylthiazoline-6-sulfonate)) and a spectrophotometer from VARIAN (Carry 100 Bio).

For the assay, 1.9 mL of 0.5 mM ABTS solution in sodium succinate buffer pH 5 and 0.1 mL enzyme solution containing 0.01 g/mL of laccase in succinate buffer pH 5 were mixed. The absorbance at 420 nm was measured immediately after adding the enzyme solution and then in an interval of 0.6 seconds. To gain the temperature profile this procedure was repeated at different temperatures. The enzyme activity was determined in units (U), where 1 U is defined as the amount of enzyme that oxidizes 1 µmol of ABTS per minute (ε_{420}=36000 M^{-1} cm^{-1} [70]).

3.2.2.2 pH profile

The enzyme activity at different pH values was determined using the plate reader from Tecan. The assay was made according to the temperature profile but for the volume of 96-well culture plates (200µl) and a laccase concentration of 0.03 g/mL.

3.3 Silicone samples

Catheters and silicone were kindly provided by DEGANIA SILICONE LTD Israel.

3.4 Sample preparation

3.4.1 Silanization

3.5 x 1.8 cm silicone stripes were prepared and washed in 5% (w/v) SDS (Sodium dodecyl sulfate) in deionized water for 30 minutes with constant stirring. After a washing cycle with deionized water and 96% ethanol (3 times), the silicone stripes were transferred into a 100 ml 5% (v/v) APTES (Amino-propyl-tri-ethoxy-silane)–ethanol solution for 1 or 24 hours. Samples were washed again and then stored in 96% ethanol.

3.4.2 Phenol- amino coupling

Gallic acid was the chemical used to provide phenols.

Stored silicone stripes were washed 3 times with deionized water and ethanol, before transferring into a 0.01 M, 0.04 M or 0.1 M gallic acid solution made with buffer (sodium-succinate buffer pH 5). 0.5 g laccase in 10 ml of the phenol solution started the reaction in a 50 ml tube at 50 °C and shaking with100 rpm. After 3or 24 hours incubation, the samples were washed 3 times and dried under nitrogen.

3.4.3 Zwitterionic surface

A 0.75 M DMAPS (Dimethyl-ammonium-propane-sulfonate) solution was used to create a zwitterionic surface. Phenolized samples were incubated in a 50 ml tube for 24 hours with 10 ml DMAPS solution (in sodium succinate buffer pH 5) and 0.5 g laccase at 50 °C and 100 rpm. Furthermore, 2 experiments were prepared with an activator (t-BHP) at 30 °C.

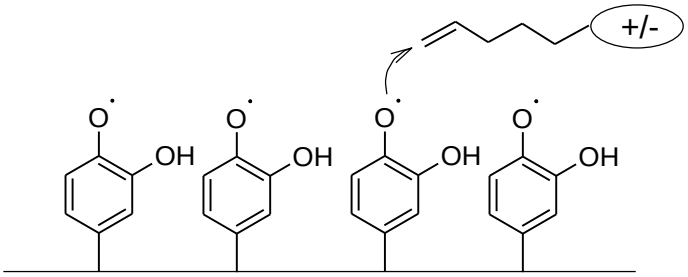

Figure 13: Proposed phenol-DMPAS coupling.
Phenolized samples were incubated for 24 h in DMAPS solution and laccase to create a zwitterionic surface.

3.4.4 Catheter preparation

Approximately 8 cm of the catheter heads were coated in the same way as described for the silicone. Only the volume of the reaction solution was increased from 10 to 45 ml.

3.5 Contact angle

Hydrophilicity was measured with a water contact angle analyzer from DSA 100 (Krüss, Germany). A water drop with a volume of 3 µl was placed on the silicone surface and the contact angle was measured using a specific software namely Krüss DSA3 v1.0.1.3-02.

On a further approach, a captive bubble contact angle method was used. The samples were placed into a vessel onto two blocs. The vessel got then filled with water and an air bubble was placed under the silicone surface. Also this air contact

angle was measured through a program. This method seems to be more sensitive than the normal water drop analysis when highly charge surfaces are analyzed.

3.6 FTIR analysis

The influence of the silanization, the phenol-amino coupling and also the DMAPS treatment was analyzed using FTIR spectroscopy from PerkinElmer (Belgium).Samples were fixed on the analyzing plate prior to measurement. Measurements were repeated 75 times to get as low noise as possible.

3.7 FITC labeling for protein attachment test

30 mL of a 2 mg/mL BSA (Bovine Serum Albumin) solution was prepared. The protein was then labeled with FITC (fluorescence isothiocyanate), purified according to the manual from Sigma and stored in the dark at 4°C.

A blank, an APTES, a GA and a DMPAS sample were then put into the labeled protein solution for 5 seconds. After drying with nitrogen, pictures were taken by a NIKON Eclipse Ti-S microscope with UV light support in order to study protein attachment on the surfaces of different sample.

3.8 Static biofilm test

An overnight culture of *Pseudomonas aeruginosa and E. coli* in a Müller Hinton broth was prepared. The optical density of both bacterial solutions was measured using a spectrophotometer from VARIAN. Then an adequate amount of cultures was transferred into sterile broth to get an OD of 0.01.

A blank, a GA and a DMAPS sample (triple test) were put into a sterile six well plate. 5 ml of the OD 0.01 bacteria solution were transferred into each well and then incubated for 24 h at 37 °C. After incubation the samples were taken out and tipped

shortly into water. Afterwards the samples were incubated for 10 minutes in 0.1 % crystal violet to stain the bacterial cells. To remove the unbound crystal violet the samples were tipped again shortly into water after the staining procedure. Then the samples were allowed to dry on air. Afterwards the stained samples were analyzed with a microscope from NIKON.

3.9 Dynamic biofilm test

An overnight culture was prepared as described in 3.8. Artificial urine was prepared according to the EN 1616 [71] with the following composition:

Table 3: Composition of artificial urine.

Urea	25g
Sodium chloride	9g
Disodium hydrogen orthophosphate, anhydrous	2.5g
Ammonium chloride	3g
Potassium dihydrogen orthophosphate	2.5g
Creatinine	2g
Sodium sulfite, hydrated	3g
Distilled water	to 1L

A 1L bottle with 500 ml of artificial urine was inoculated with *Pseudomonas aeruginosa* to an OD of 0.1. A coated and a blank catheter were plugged on a tube splitter which then was plugged on the lid of the bottle. The tube which was going out of the lid was then connected to a peristaltic pump and back to the bottle. According to EN 1616 the pump was adjusted to 1mL/min/catheter. All tubes were from the catheter itself. The whole setup could be autoclaved. In a second setup also 0.3 g of $MgCl_2$ and 0.49 g of $CaCl_2$ were added to test the antifouling properties.

3.10 XPS (x-ray photoelectron spectroscopy) analysis

Samples were cleaned with deionized water, dried under nitrogen. The XPS analysis itself was performed at the University of Barcelona.

4. Results and discussion

4.1 Enzyme concentration

In order to measure the concentration of the laccase a calibration curve was created (see figure 14) according to the user manual of the Bicinchoninic Acid Kit (SIGMA).

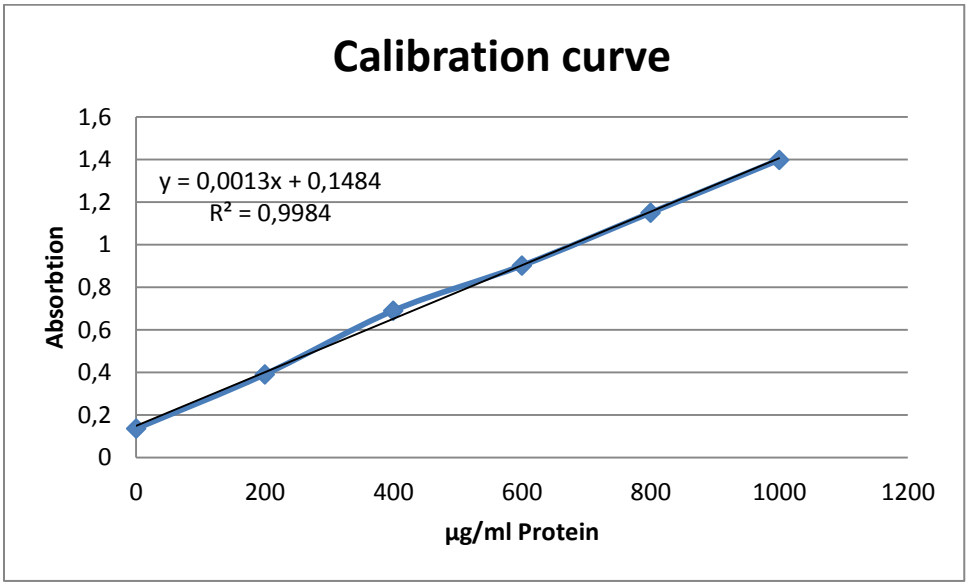

Figure 14: Calibration line with BSA for the calculation of the enzyme concentration.

All protein dilutions were prepared in triplicate. An average of all measurements led to a concentration of ~ 0.67 mg/ml for the DENILITE IIS Laccase.

As 8 mg/ml were weighed in, this means that only ~**8.38 %** of the powder is enzyme.

4.2 Enzyme activity

4.2.1 pH profile of DENILITE IIS laccase

The enzyme activity at different pH values was measured.

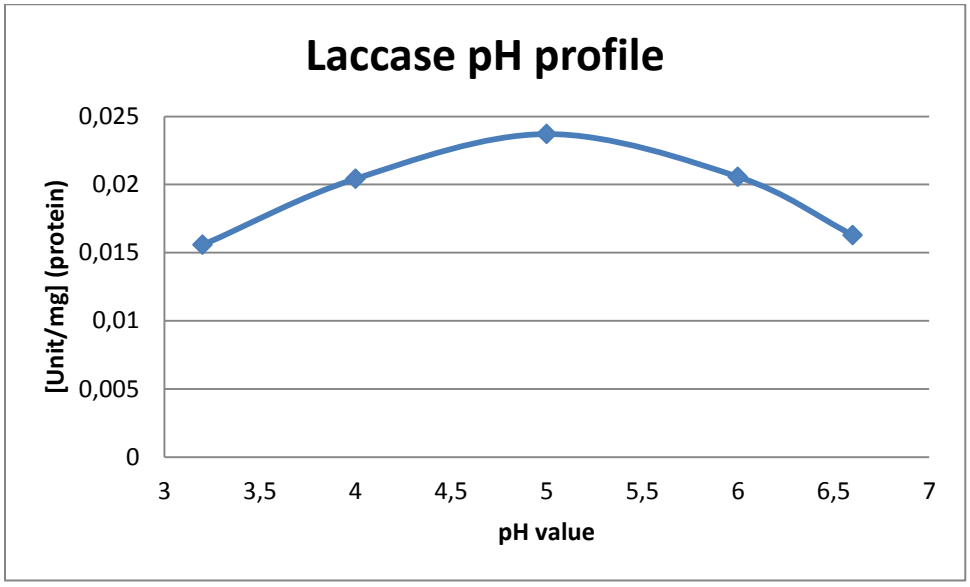

Figure 15: pH profile of DENILITE IIS laccase.

The enzyme activity was calculated using the following formula.

$$U = \frac{\Delta abs \times Vtotal \times f}{VEnzyme \times d \times \varepsilon}$$

Formula 4: Enzyme activity calculation.

Δabs: rise of de laccase activity at the different pH (min^{-1})

V_{total}: volume of one plate cell (220 µl)

f: dilution factor: 1

V_{enzym}: amount of enzyme (110 µl)

d: thickness of the well (0.61 cm)

E: extinction coefficient (36000 $l*mol^{-1}*cm^{-1}$)

The best activity of the laccase solution at room temperature was calculated at pH 5 and is **0.023 U/mg** (protein).

4.2.2 Temperature profile of DENILITE IIS laccase

The enzyme activity at different temperatures was measured.

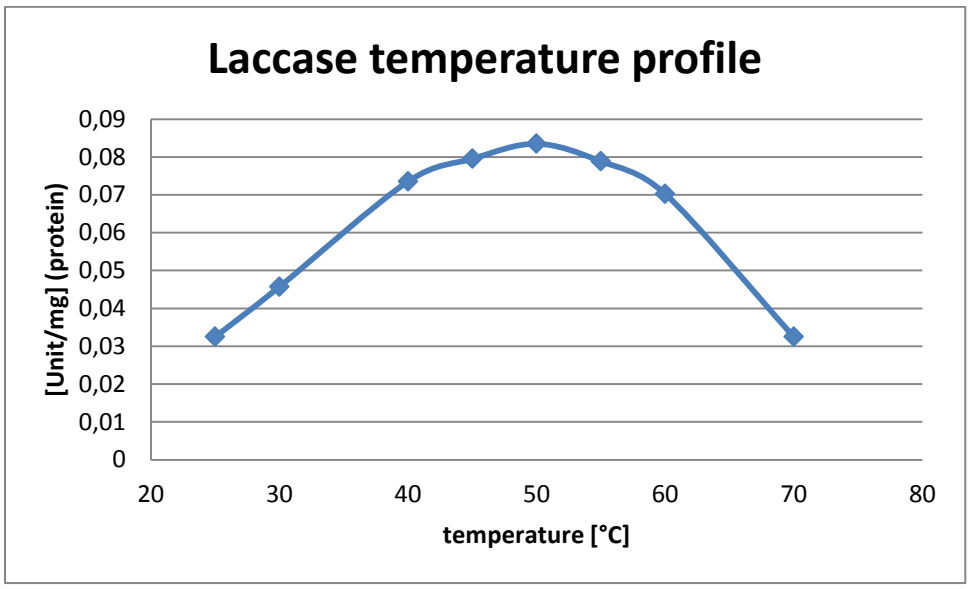

Figure 16: Temperature profile of DENILTE IIS laccase

The enzyme activity was calculated using the following formula 4.

$$U = \frac{\Delta abs \times Vtotal \times f}{VEnzyme \times d \times \varepsilon}$$

Δabs: rise of de laccase activity at the different pH (min^{-1})

V_{total}: volume of the cuvette (2 ml)

f: dilution factor: 1

V_{enzym}: amount of enzyme (0.1 ml)

d: thickness of the cuvette (1 cm)

E: extinction coefficient (36000 $l*mol^{-1}*cm^{-1}$)

The best activity of the laccase solution at pH 5 was calculated at 50°C and is **0.083 U/mg** (protein).

4.3 Silanization of the silicone samples

The silanization was made to provide amino groups on the silicones surface for further experiments. After the incubation (1 h and 24 h), the samples were washed and dried under nitrogen. Following tests were performed:

FTIR was used to see differences between the silanized and a blank sample. Primary, secondary and tertiary amino groups should be seen at 3222, 2666 and 2631cm^{-1} [72]. Unfortunately there was no significant difference at the FTIR peaks detectable.

One possible explanation could be that the FTIR is not sensitive enough to show any differences because the layers are too thin. We didn't get any results from the composition of the silicone, but we believe that there are less OH groups on the surface, where the silane is able to covalently bind to the surface.

For verification a test with a 2 % ninhydrin solution was performed. This reagent couples with the amino groups and a dark purple color, called Ruhemanns purple, appears [73]. Figure 17 shows the chemical structure of ninhdydrin.

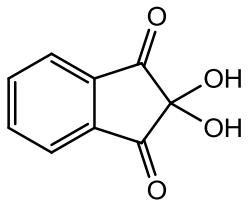

Figure 17: Chemical structure of ninhydrin.

1 h and 24 h samples showed dark purple color, which is an evidence for amino groups on the surface (see figure 18). Even the 24 h sample was a little bit purpler than the one of 1 h. Due to this fact the silanization reaction was set to 24 hours for further experiments, to be sure that enough amino groups were provided on the surface.

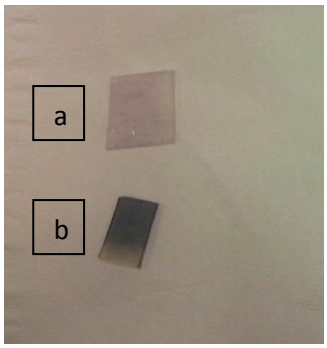

Figure 18: Ninhydrin test on silanized sample. a: blank without color, b: sample that showed dark purple color due to the amino groups on the surface

4.4 Lacasse mediated amino-phenol coupling

After treatment the samples were washed with deionized water and ethanol and dried under nitrogen. After a 3 h reaction the solution containing 0.01 M gallic acid showed a slightly brown color. This indicates a low polymerization rate of gallic acid, which leads to the assumption, the amount of gallic acid was too low.

The experiment with a higher concentration of gallic acid (0.1 M) showed quite the same color. This could be due to an enzymatic inhibition caused by a high phenolic radical concentration.

The highest polymerization grade was reached with 0.04 M gallic acid solution where a dark brown color appeared. This is in agreement with previously published results [74]. An increased reaction time showed a darker color on the surface but this is also an evidence for a higher grade of oxidation of the gallic acid. This means that less OH groups would be left for the next coupling reaction. Consequently, the 24 h experiments showed bad results in the subsequent experiments and the phenolization step was set to 3 h for all further experiments.

Also at the silicone samples a light brown color could be observed which led to the assumption that the (polymerized) phenols were attached to the surface (figure 19).

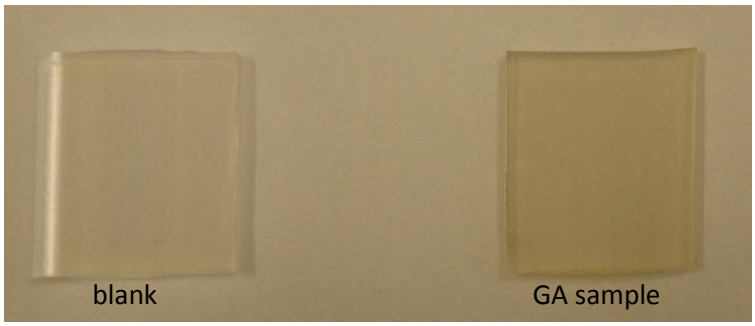

Figure 19: Blank silicone compared with a phenolized sample.
The GA sample showed a light brown color compared to the blank. This led to the assumption that the (polymerized) phenols were attached to the surface.

FTIR was used to see differences between the phenolized and a blank sample.

Again there didn't appear any significant differences between the phenolized sample and the blank. It is difficult to analyze the phenolized samples by FTIR, because the silicone itself shows big peaks in the same region where the phenols could appear. As also mentioned in 4.3, we consider that only few amino groups are provided on the surface and so only a couple of phenols were able to bind.

After putting the sample in a 0.02 mM DPPH-methanol solution the violet color disappeared, which demonstrates an antioxidation reaction. In fact phenols are antioxidants which is a proof of that the amino phenol coupling could be achieved.

Another ninhydrin test was performed to prove the phenol coupling on the surface. The samples appeared purple, but even less than the blanks (APTES treated silicone). This could mean that the phenols were coupled to the amino groups, but only a small amount, which would explain the FTIR results as well.

4.5 Zwitterionic surface

After the 24 h treatment, the samples were washed with water and dried under nitrogen. The samples appeared reddish (figure 20) after the treatment which led to the assumption, that the reaction worked as supposed. The samples made with t-BHP as an activator didn't show as good visual results as the laccase mediated ones. Therefore the t-BHP activator was not used anymore in the further experiments. It is supposed that the peroxide used to activate the DMAPS coupling inactivated the laccase. Nevertheless this would have been just a chemical proof if it had worked.

After 48 h the reaction solution containing DMAPS monomers and laccase in presence of the gallic acid samples gelled, which proved a polymerization of the DMAPS. The acrylic zwitterionic monomer is not a suitable substrate for the laccase, so the only possible explanation for the gelation is that the enzyme created oxygen radicals from the OH groups provided by the phenols. These radicals might break the CH_2=CH bond of the DMAPS, initiate a polymerization and promote the direct bonding to the oxygen from the OH group itself.

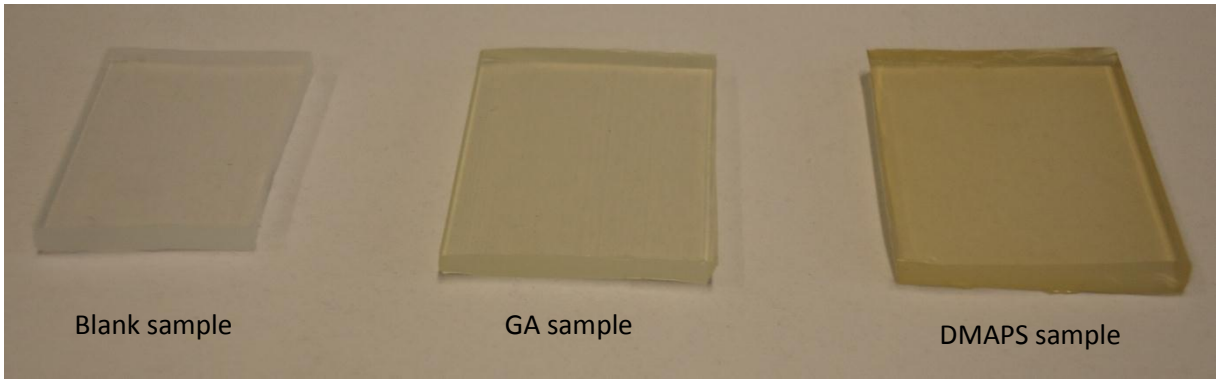

Figure 20: Comparison between a blank, GA and DMAPS sample.
The DMAPS sample appeared reddish compared to the blank and the GA sample which led to the assumption that the reaction worked as supposed.

4.6 Water contact angle

The results of the water contact angle measurements are shown in the following table (table 4) and figure (figure 21).

Table 4: Water contact angle.

Samples	Water contact angle (average)	
	Left angle	Right angle
Blank	106,3°	106,7°
APTES	109,5°	108,8°
GA	101,8°	102,6°
DMAPS	99,8°	97,2°

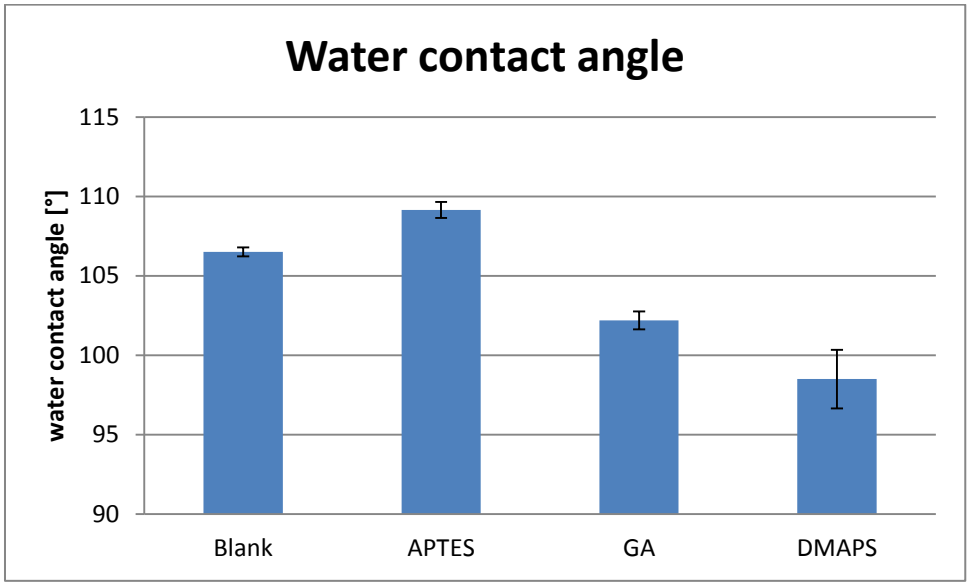

Figure 21: Water contact angle of a blank, APTES, GA and DMAPS sample.
The differences in the water contact angle between the samples were not significant. A reason could be that this method is not sensitive enough for these thin coatings.

The water contact angle measurements gave no significant result and led to the conclusion, that the coatings were too thin to change the angle of a water drop.

That's why the more sensitive method of captive bubble contact angle was performed. The following table (table 5) shows the measured values.

Table 5: Air contact angle.

Samples	Air contact angle (average)	
	Left angle	Right angle
Blank	79,6°	75,7°
APTES	78,7°	78,8
GA	45,3°	45,5°
DMAPS	43,1°	42,9°

The results in table 5 and figure 22 show a very low air contact angle for the GA and DMPAS samples. This makes perfect sense because gallic acid has 3 OH groups on each aromatic ring, which makes the surface hydrophilic. Even the DMAPS samples have a little lower angle than the GA samples which shows that the DMAPS coupled to the phenols [67].

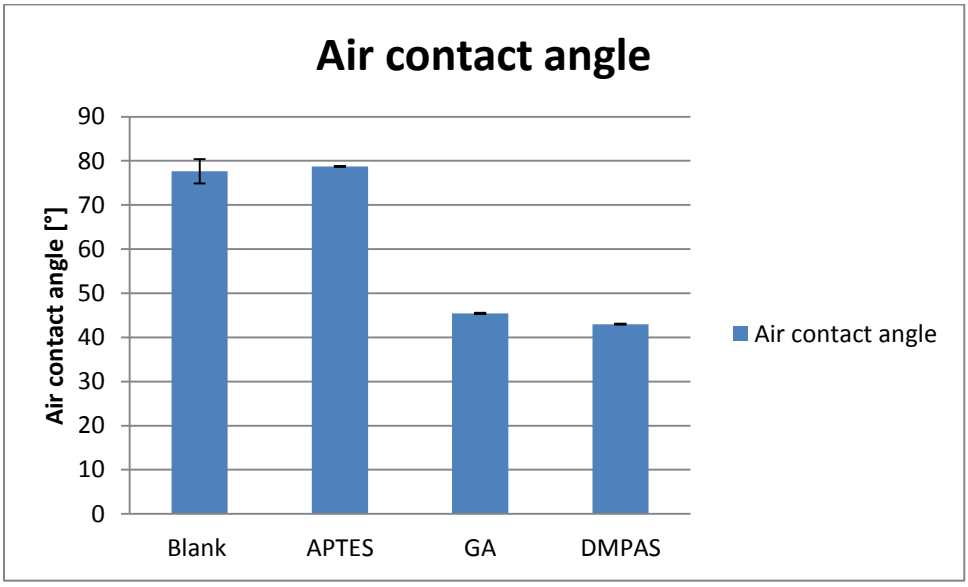

Figure 22: Air contact angle of a blank, APTES, GA and DMAPS sample.
The air contact angle of the GA and DMAPS samples was very low compared to the blank and APTES samples. The 3 OH groups on each aromatic ring of the GA are the reason for this hydrophilic surface. The angle of the DMAPS sample was a little bit lower than the angle for the GA sample. This shows that the DMAPS coupled to the phenols, as it is more hydrophilic.

The lower angle of DMAPS compared to the GA samples, is a sign for the accomplished coupling of DMAPS to the phenols.

The unexpected low contact angle of the silicone samples (which are hydrophobic) was probably due to the presence of some remaining surfactant used in the washing step.

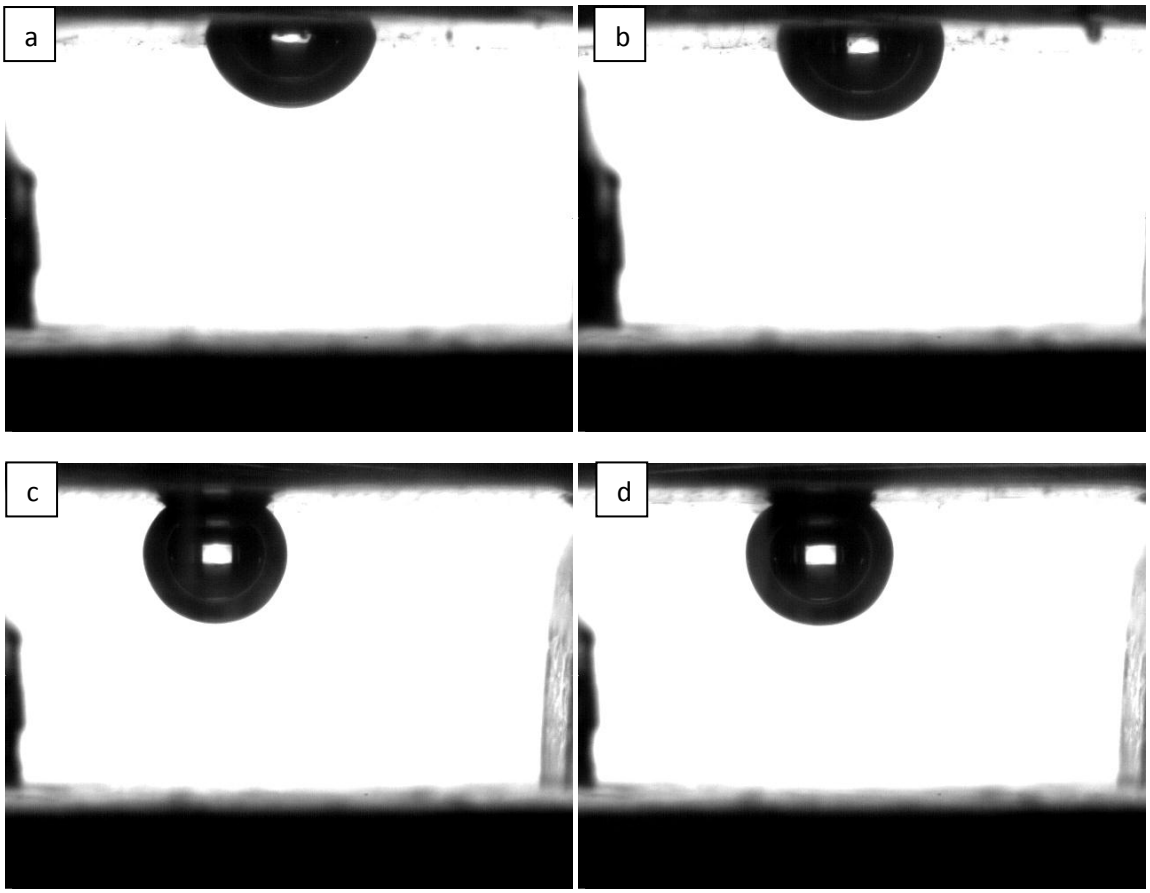

Figure 23: Air contact angle measurement.
a: blank sample, b: APTES sample, c: GA sample, d: DMAPS sample.

4.7 XPS analysis

XPS analysis was made for a blank, an APTES, a GA and a DMPAS sample to verify the previous results. The following figures show some specified high resolution peaks of the different samples.

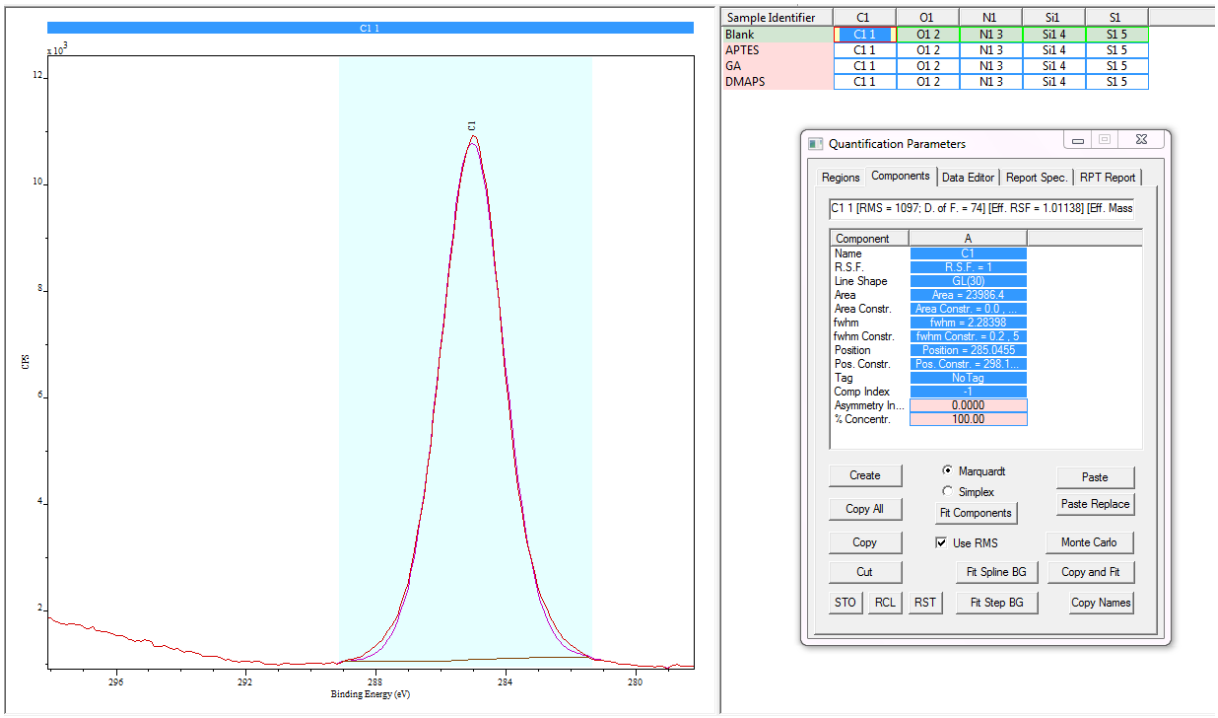

Figure 24: High resolution C1s peak of a blank sample made by XPS analysis.

The C1s peak, characterized by an energy emission at 285.2 electron volt (eV), can be ascribed to carbon bonded to either hydrogen or another carbon atom [75] [76] (see figure 24). Unfortunately, we didn't get the analysis of the silicone itself till now, so a better comparison between the XPS analysis and the silicone itself cannot be done yet.

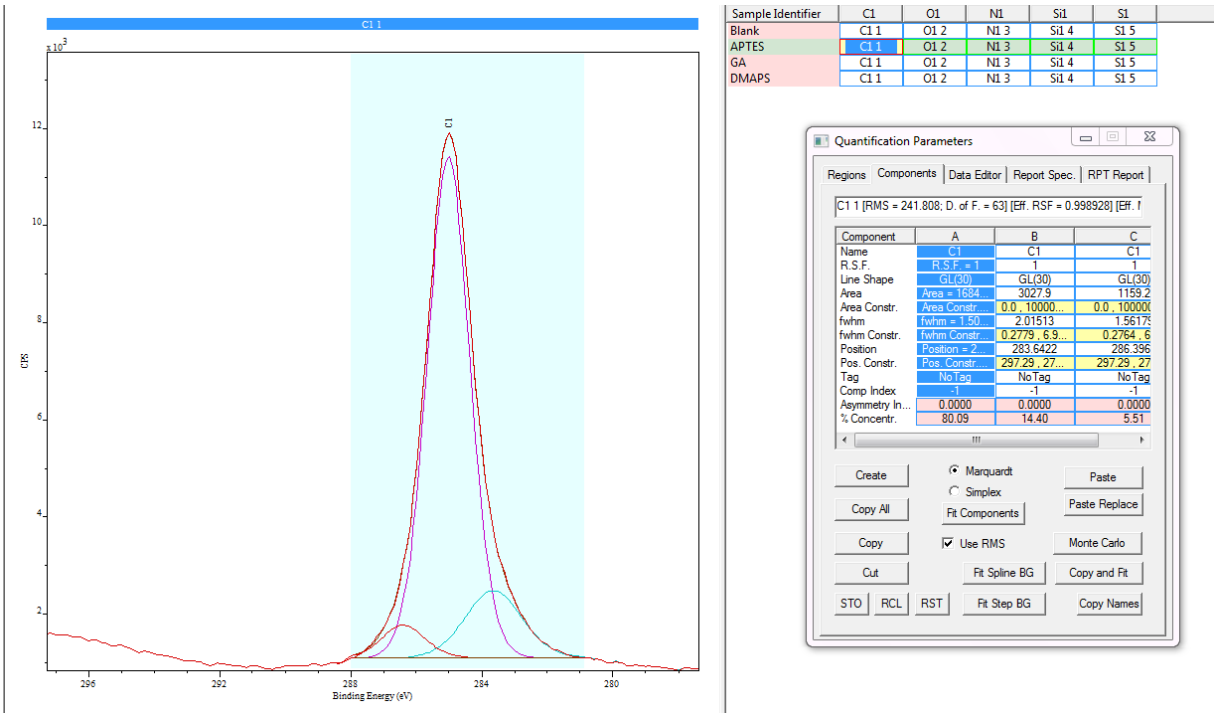

Figure 25: High resolution C1s peak of an APTES sample made by XPS analysis.

Figure 25 shows the high resolution C1s peak of an APTES sample. In comparison to the blank sample, two new peaks appeared. One at ~284 eV and a second one at ~286,6 eV. The peaks at 285.2 and 286.6 eV are common to all alkylated and H-terminated Si surfaces [77], whereas the low binding energy peak at 284.0 eV is unique to alkylated Si surfaces. Hence, the first peak at 284.0 eV can be assigned to emission from core-level electrons of carbon atoms covalently bonded to the relatively electro-positive silicon (C-Si) [78] [79]. Another possible explanation for the ~286,8 eV peak could be the N^{+}-C bond [75] which would also make sense, due to the fact that APTES consists of an Si-C-NH_3 bond.

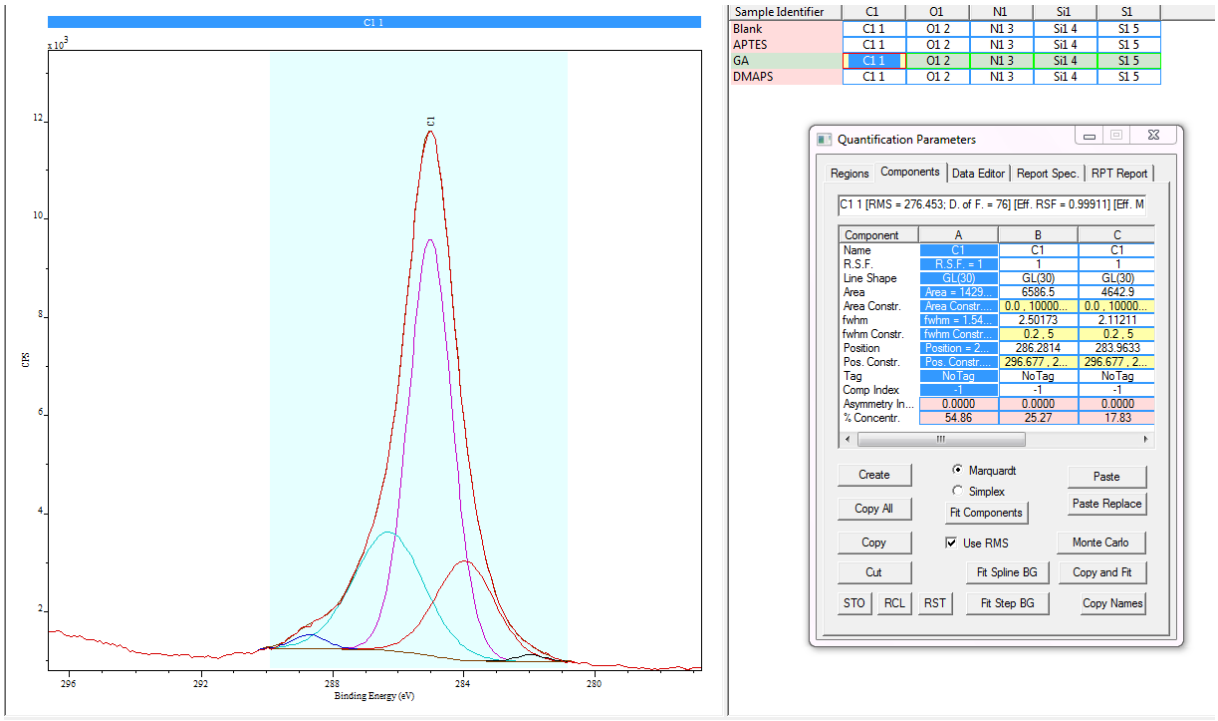

Figure 26: High resolution C1s peak of a GA sample made by XPS analysis.

In comparison to the APTES sample, only one new C1s peak at ~289 eV appeared at the GA sample (see figure 26). This peak is suggested to be from a carboxylic group, which would make perfect sense in relation to the carboxylic group of gallic acid [75].

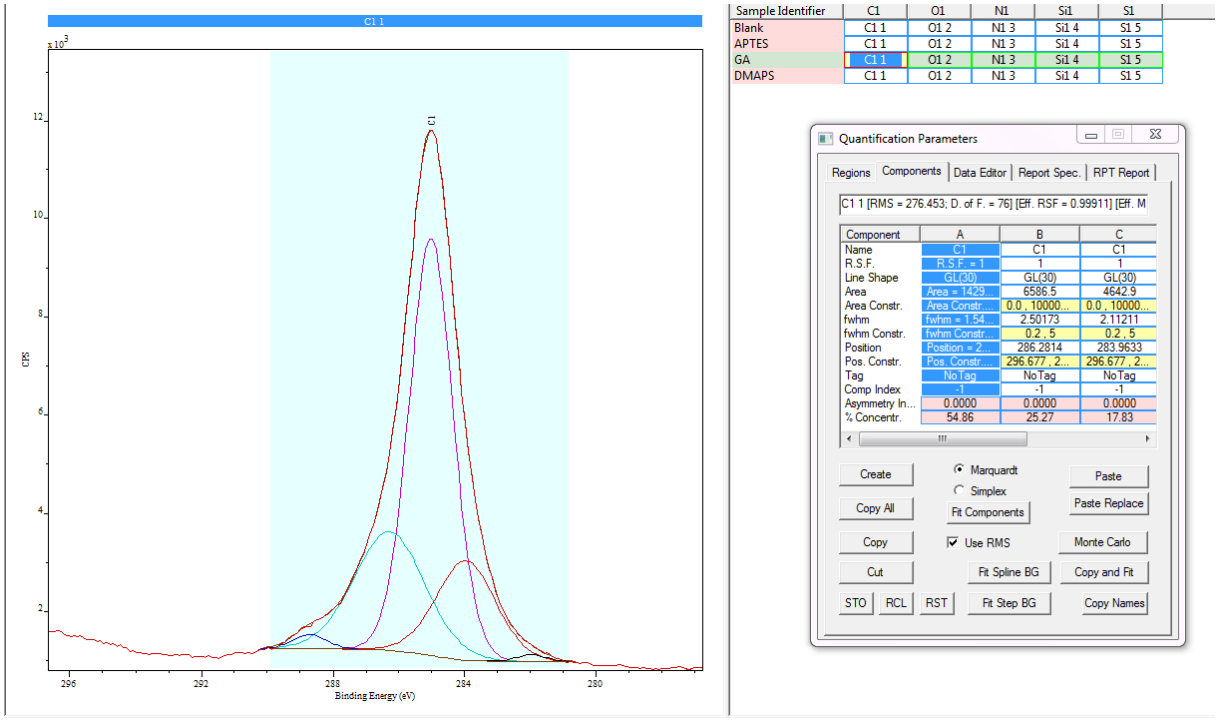

Figure 27: High resolution C1s peak of a DMAPS sample made by XPS analysis.

In figure 27 the high resolution C1s peak of a DMAPS sample is shown.

No real differences can be seen between the C1s peaks of the GA and the DMAPS sample. Probably the C bonds to the other atoms in the molecule of DMAPS are quite similar to the previous couplings. Therefore, the peaks should be at the same range of eV, so the DMAPS peaks may be “hidden”.

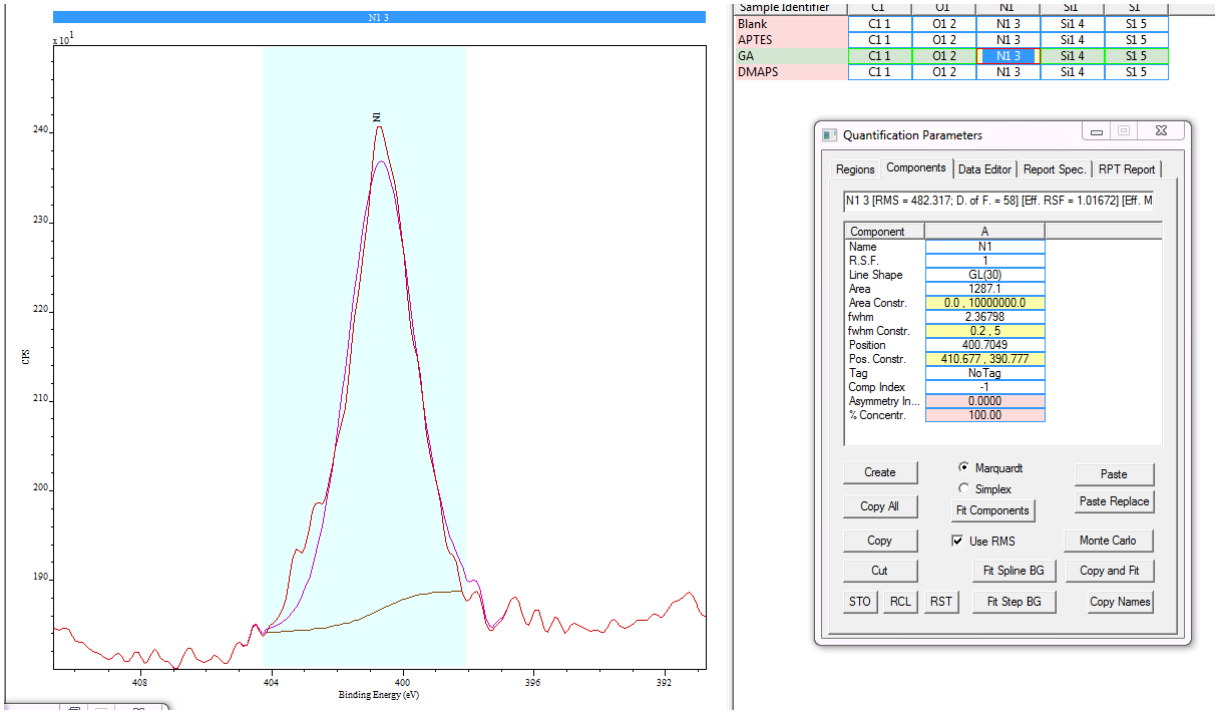

Figure 28: High resolution N1s peak of a GA sample made by XPS analysis.

The GA N1s peak appeared at ~400.2 eV (see figure 28) which is described as a protonated amino group (NH_3^+) [80]. This would add up to the fact, that the amino group of APTES is protonated at a pH lower than 11. Another paper suggests that this can also describe a N-COO group [75].

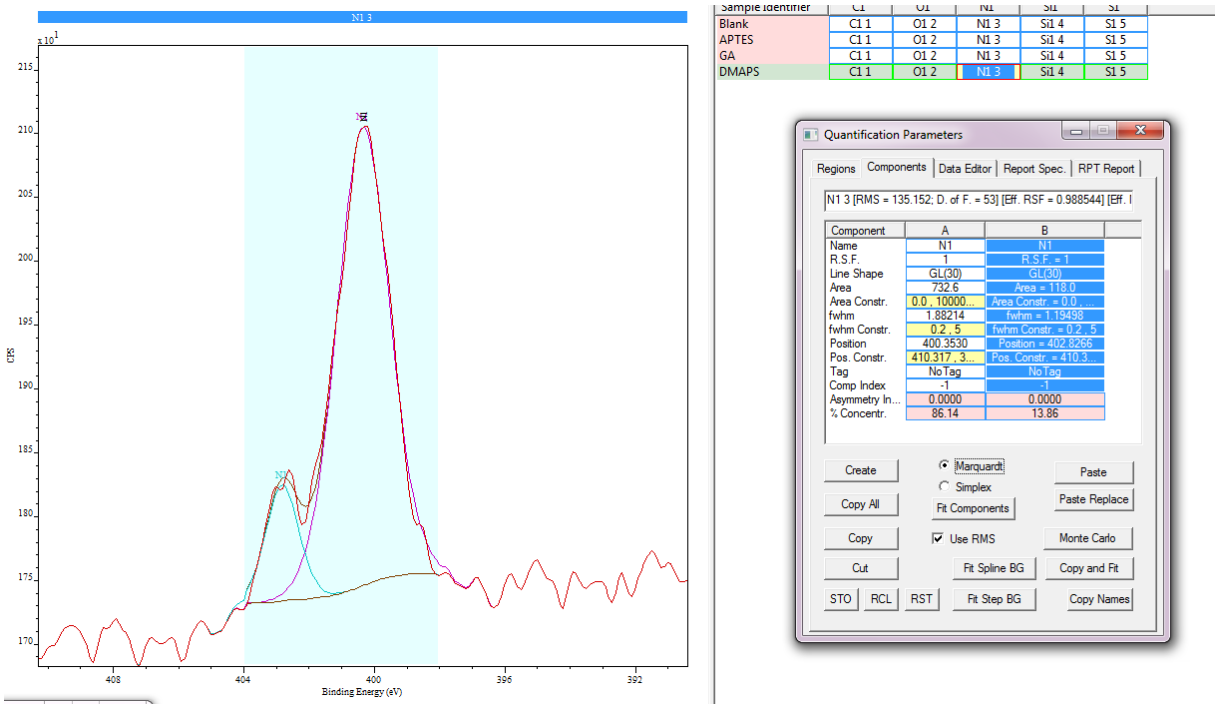

Figure 29: High resolution N1s peak of a DMAPS sample made by XPS analysis.

Figure 29 shows the N1s peak of a DMAPS sample made by XPS analysis. The high resolution N1s picture of DMAPS showed a second peak at ~403.4 in comparison to the GA N1s peak. This peak is described as a ammonium nitrogen ($–N^{+}(CH3)_3$) at 403.45 eV [75] which would perfectly fit for the nitrogen in the DMAPS structure.

Unfortunately the XPS results came very late and therefore it was not possible to show or even interpret all results. Nevertheless, the previous high resolution pictures showed a clearly that the coating worked as supposed.

The following table 6 and figure 30 show the desired analyzed atoms from XPS analysis and their percentage in the samples.

Table 6: XPS calculated composition of 4 different samples.

	C1s	N1s	O1s	Si2p	S2p
Blank	49.44	0.00	24.12	26.44	0.00
APTES	50.00	0.41	23.97	25.62	0.00
GA	52.87	1.90	24.98	20.26	0.00
DMAPS	53.45	1.24	23.35	21.47	0.49

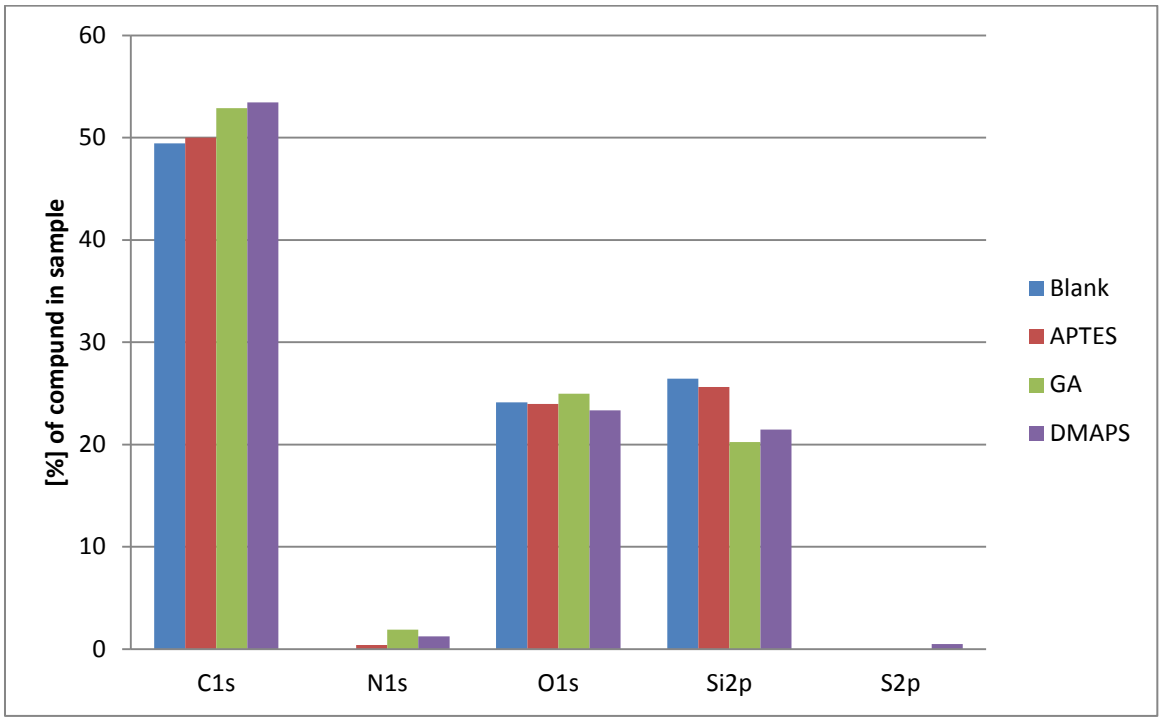

Figure 30: XPS analysis from a blank, APTES, GA and a DMAPS sample.

By XPS analysis clear results were obtained. All samples showed lower values for the Si2p peak in comparison with the blank, which is a proof for the successful coating of the silicone samples.

The percentage of C1s atoms was higher at the GA and DMAPS sample as these two chemicals provide carbon atoms in their chemical structure. Additionally the percentage of the Si2p atoms declined, which proves that the silicone was getting coated. Although the slight decline suggests that the coating is in a nm range.

The high O1s percentage of the GA sample can be explained by the chemical composition of gallic acid, which contains three OH- and one carboxyl- group. Also the amount of O1s decreased in the DMAPS sample because there is no oxygen in the chemical structure.

Also the N1s peaks show clearly that the silanisation was successful. It's not yet clear why the GA has the highest N1s peak, but further investigations have to be done. Anyhow, the DMAPS sample showed a higher amount of nitrogen than the APTES sample which can be explained by the nitrogen in the zwitterionic molecule itself.

Due to the fact, that the zwitterionic DMAPS is the only molecule used for coating which has sulfur in its structure, it can be concluded, that the coating worked as supposed.

4.8 Protein attachment test

To prove the antifouling property of the coated silicone surface, BSA was labeled with FITC. The samples were dipped for 5 seconds in a solution containing the FITC labeled BSA. After drying under nitrogen the attached protein could be seen in the microscope provided with UV light:

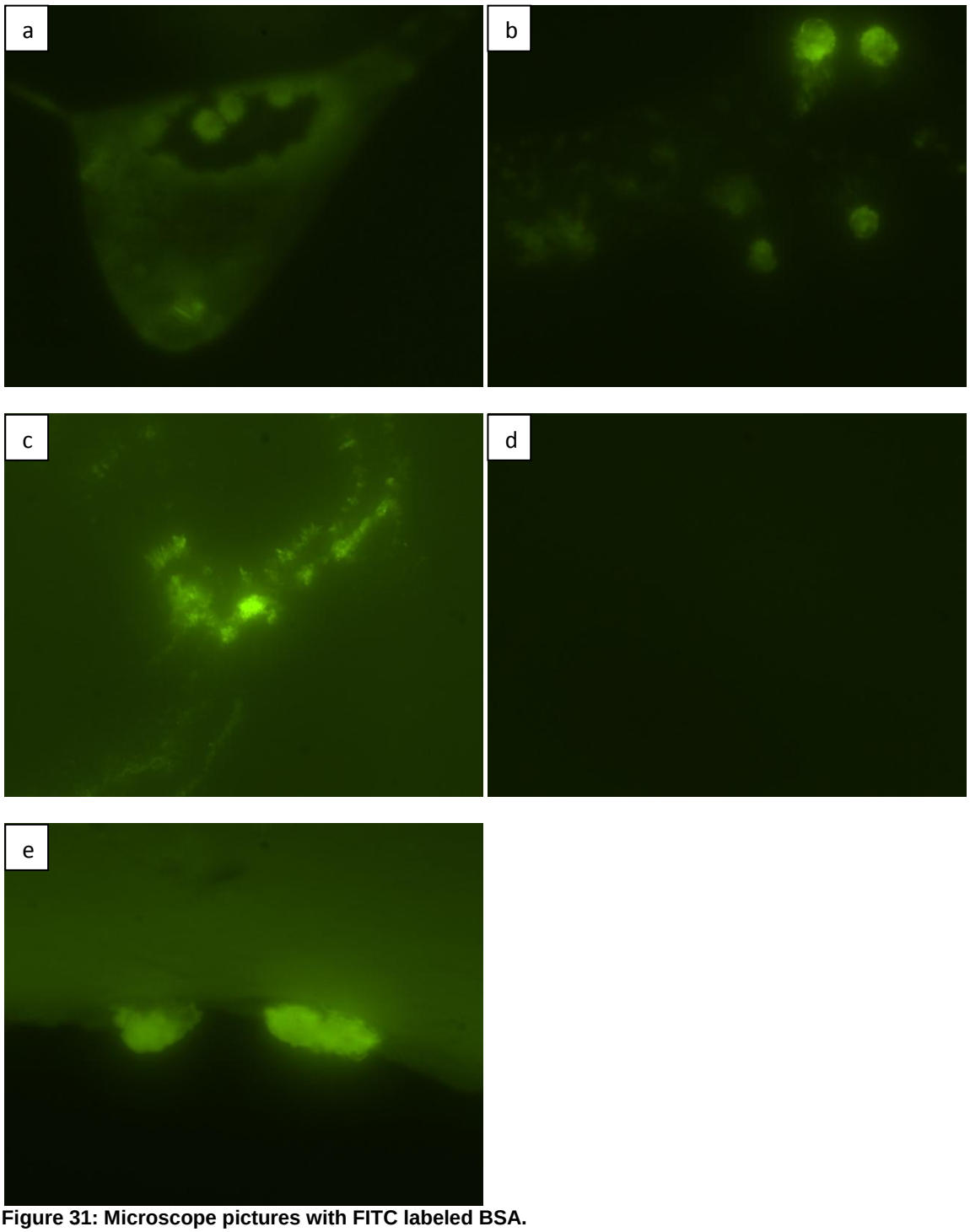

Figure 31: Microscope pictures with FITC labeled BSA.
A: blank sample, b: APTES sample, c: GA sample, d: DMAPS sample, e: the edge of a DMAPS sample.

All samples showed proteins attached to the surface, except for the DMPAS sample (figure 31). This proves the anti-fouling property. Picture D was a DMAPS sample which was cut in the middle after coating it. So there was no coating on the edge of the sample and the attachment of protein can be seen in this edge (picture E).

4.9 Static biofilm test

In order to show the ability of the coating to inhibit biofilm formation a static biofilm test was made with *Pseudomonas aeruginosa*. After 24 h incubation the samples were analyzed using a microscope (see the following figure 32).

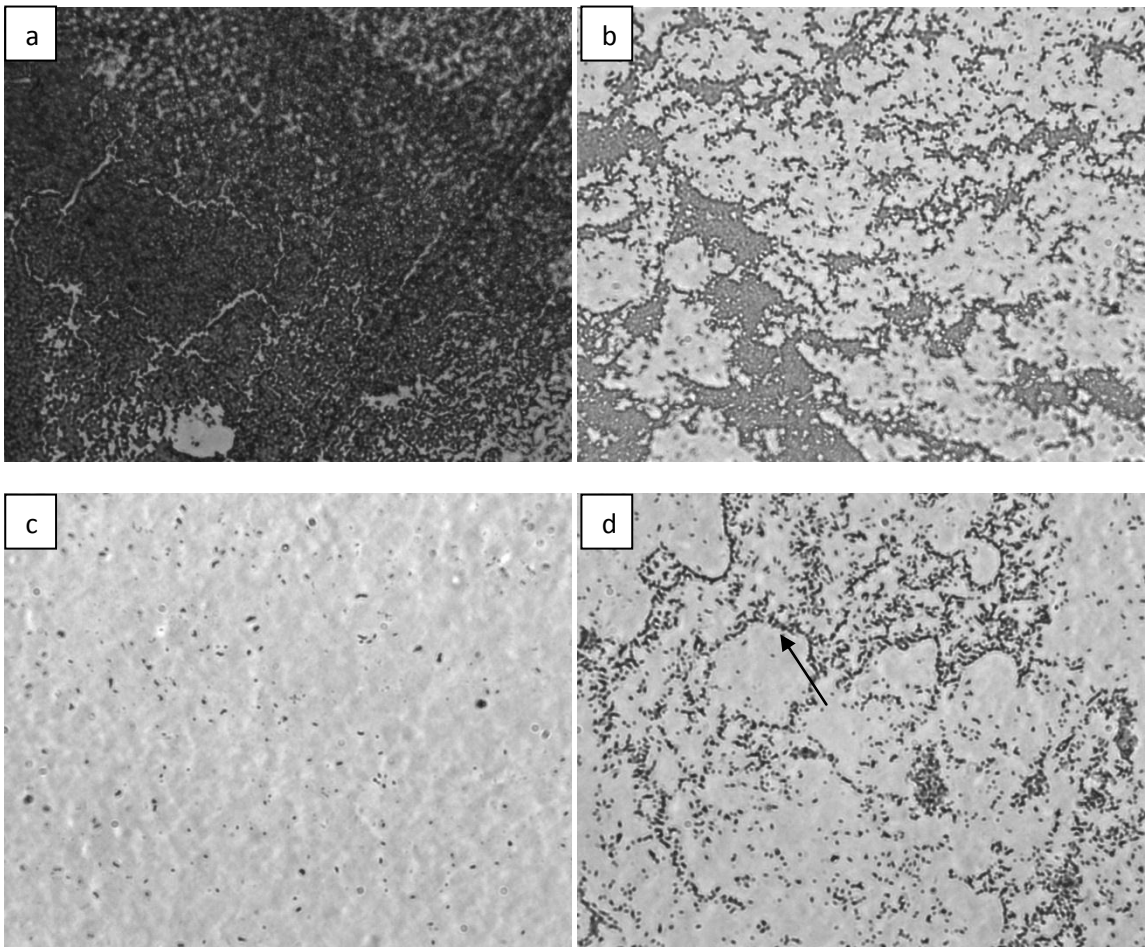

Figure 32: Microscope pictures of the static biofilm test with *Pseudomonas aeruginosa* after 24h. objective: x40 ;a: blank sample, b: GA sample, c and d: DMPAS sample on different positions. It can be clearly seen, that the blank sample has more bacterial growth compared to all other samples.

It can be clearly seen, that the blank sample (a) was full of bacteria. The different nuances in the brightness of the bacteria indicate different heights. The bacterial formation can be considered as a three-dimensional structure and therefore as a biofilm. In contrast the gallic acid sample (b) has still a lot of bacteria on the surface. But they seem to be all in one level which leads to the conclusion that the biofilm formation didn't start yet. DMAPS pictures show two different sites which are not antithetic. On the one hand (c) there are only few bacteria on the surface which

proves the nonfouling and antibiofilm surface properties of the sample. On the other hand (d) there are more bacteria than in (c). But these boarders of a dried water drop (arrow in the picture shows one) indicates that the short washing step wasn´t able to wash all bacteria away. This leads to the assumption that the bacteria were not able to firmly adhere to the surface.

The same test was also performed with *E. coli.* The following microscope pictures (as seen in figure 33) could be obtained.

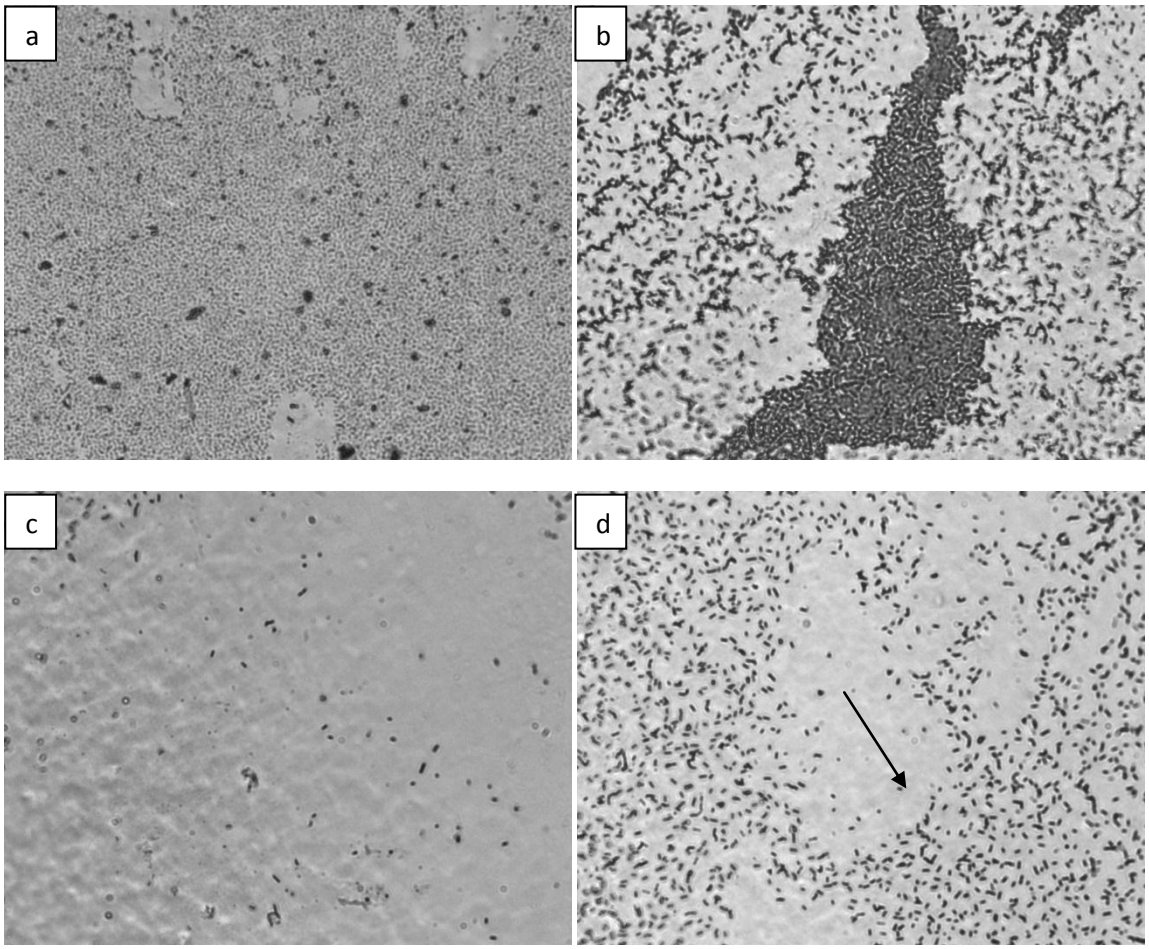

Figure 33: Microscope pictures of the static biofilm test with *E.coli* after 24h.
objective: x 40; a: blank sample, b: GA sample, c and d: DMPAS sample on different positions. The blank showed a lot of bacteria, the GA sample seems to have better antibiofilm properties against *P. aeruginosa* than *E. coli*, but the DMAPS sample again showed good antibiofilm properties.

The static biofilm test with *E.coli* showed similar results as the one with *P. aeruginosa*. The blank sample (a) showed again a lot of bacteria. The light color of *E coli* in the picture indicates a different height level of the formed biofilm. Also the gallic acid sample (b) shows bacterial structures with different heights. The antibiofilm properties of gallic acid seem to be more effective for *P. aeruginosa* than for *E. coli* [81]. The DMAPS samples are clearly similar to the one in figure 32 and show again good antibiofilm properties.

4.10 Catheter coating

The catheter heads were coated in the same way as the silicone samples and showed following results (see figure 34).

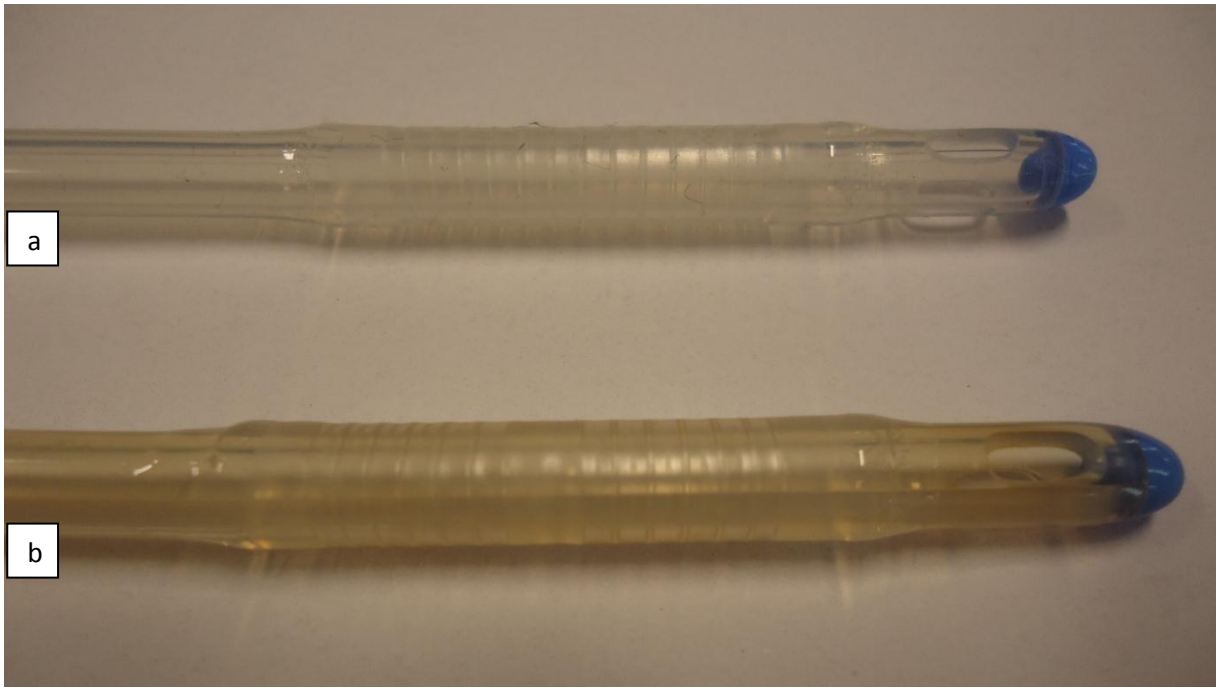

Figure 34: Coated catheter (b) compared with a normal one (a).
Color differences between the blank and the coated catheters can be seen similar to the silicone samples. This led to the conclusion that the coating also worked for the catheters.

In figure 34 color differences of the catheters can be seen similar to the silicone samples which led to the conclusion that the coating worked perfectly. As the catheters have an eye hole, the reaction solution could enter the tube so the catheters are also coated inside.

4.11 Dynamic biofilm test

A dynamic biofilm test was prepared to test the antibiofilm and antifouling coating on the catheters.

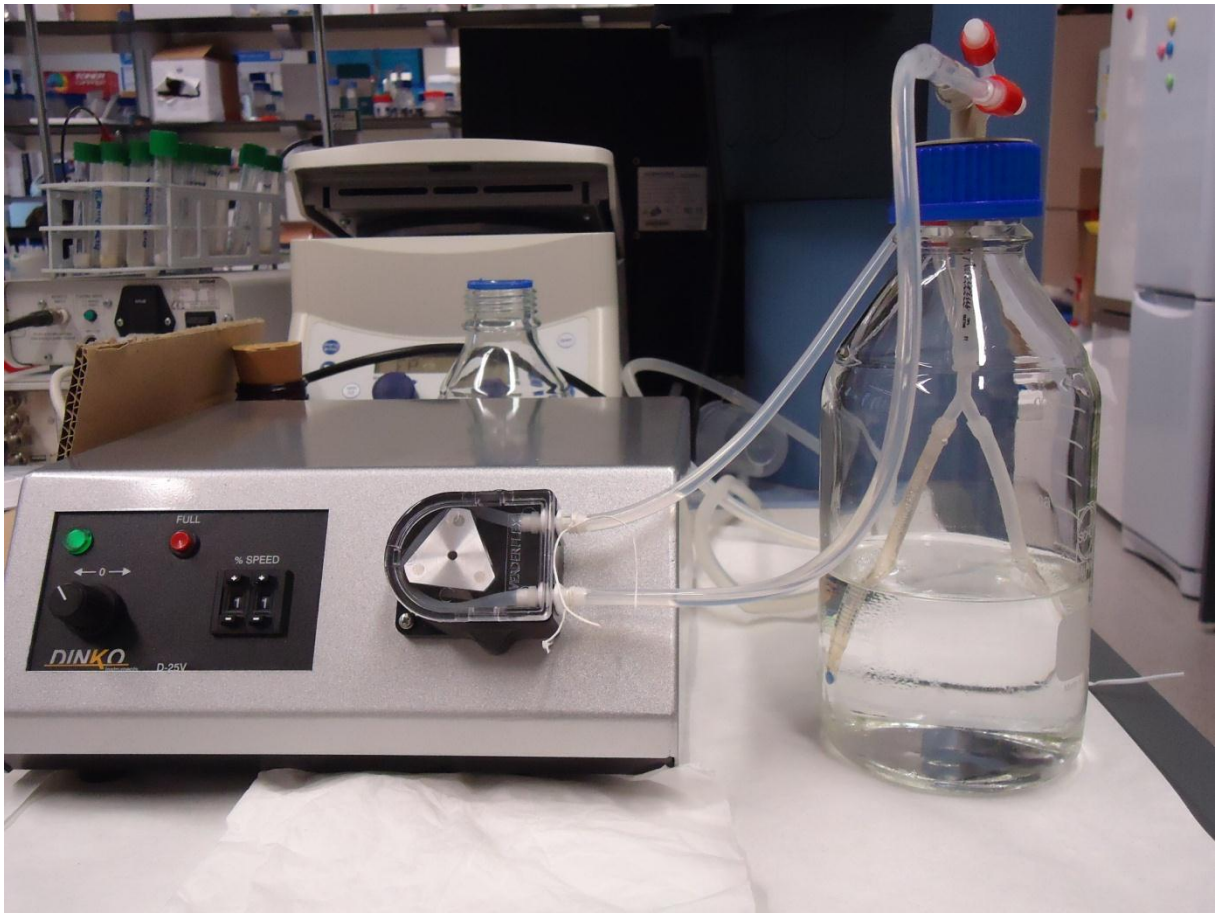

Figure 35: Experimental setup for a dynamic biofilm test.
Artificial urine was inoculated with *P. aeruginosa* and the liquid was pumped through the system with 1 ml/min for each catheter (one blank and one coated).

After 1 week the experiment was stopped. Unfortunately there was no change visible on the surface. The solution itself didn‘t change as expected due to the inoculation of the bacteria. Also the catheters themselves were clean. Even after rising of the pH to 8, which should lead to a fall out of magnesia and calcium chloride, no results were obtained.

Bacteriological analysis has subsequently confirmed that the urease producer *Proteus mirabilis* is the predominant organism in encrusted catheter biofilms [82], so further experiments should include this organism.

5. Conclusion and outlook

In this master thesis an antibiofilm and antifouling coating on pre-aminated silicone urinary catheters was established enzymatically by grafting natural polyphenols with known antimicrobial activity onto silicone followed by the introduction of zwitterionic moieties.

The silanization reaction with APTES and the subsequent covalent binding of the functional group was proven with the ninhydrin solution test. In addition, XPS analysis showed a clear amino peak which is another proof for the presence of APTES on the surface.

The DPPH test made clear, that phenols were present on the surface and that they retained their antioxidant activity. Also the water contact angle measurement showed a lower contact angle indicating a higher number of OH groups on the surface. Even the static biofilm test verified a lower biofilm formation compared to the blanks. Although there were no differences detectable by FTIR, XPS analysis gave the evidence of a higher percentage of carbon and oxygen.

Changes of the zwitterionic surface properties could be proven with different methods as well. The water contact angle measurement showed a smaller angle then the phenolic surface because of the more hydrophilic properties of DMAPS. The static biofilm test as well as the FITC coupled BSA test showed an anti- attachment surface for bacteria or even proteins. XPS showed a clear sulfur peak, which is also a proof of the zwitterionic surface.

Unfortunately the FTIR analysis gave no results which can be explained by the very thin layers that are presumed somewhere in the nano-region.

It can be concluded, that the coatings described in this thesis worked very well. Although the different layers are only in a nano-region, very good results have been obtained.

Anyway, more experiments have to be done to verify the antibiofilm and antifouling properties, to properly go on to the next steps like cytotoxicity tests or even human trials. Also leaching tests that prove the stability of the coating should be done.

6. List of figures, tables and formulae

7. References

[1]. **Saint, S. and Chenoweth, C.E.** Biofilms and catheter-associated urinary tract infections. *Infectious Disease Clinics of North America.* 2003, 17(2): 411-32.

[2]. **Tambyah, P.A. and Maki, D.G.** Catheter-associated urinary tract infection is rarely symptomatic: a prospective study of 1,497 catheterized patients. *Archives of Internal Medicine.* 2000, 160(5): 678-682.

[3]. **Choong, S., et al.** Catheter associated urinary tract infection and encrustation. *International Journal of Antimicrobial Agents .* 2001, 17(4):305-10.

[4]. **Tenke, P., et al.** The role of biofilm infection in urology. *World Journal of Urology.* 2006, 24(1): 13-20.

[5]. **Aksoy, A.E., Hasirci, V. and Hasirci, N.** Surface Modification of Polyurethanes with Covalent Immobilization of Heparin. *Macromolecular Symposia.* 2008, 269(1): 145–153.

[6]. **Yang, S.H., et al.** Chitosan/poly(vinyl alcohol) blending hydrogel coating improves the surface characteristics of segmented polyurethane urethral catheters. *Journal of Biomedical Materials Research Part B: Applied Biomaterials.* 2007, 83(2): 304-13.

[7]. **Fu, J., et al.** Construction of anti-adhesive and antibacterial multilayer films via layer-by-layer assembly of heparin and chitosan. *Biomaterials.* 2005, 26(33): 6684-6692.

[8]. **Rose, S.F., et al.** Bacterial adhesion to phosphorylcholine-based polymers with varying cationic charge and the effect of heparin pre-adsorption. *Journal of Materials Science: Materials in Medicine.* 2005, 16(11): 1003-1015.

[9]. **Shi, L, et al.** Mucin coating on polymeric material surfaces to suppress bacterial adhesion. *Colloids and Surfaces B: Biointerfaces.* 2000, 17: 229–239.

[10]. **Eydelnant, I.A. and Tufenkji, N.** Cranberry derived proanthocyanidins reduce bacterial adhesion to selected biomaterials. *Langmuir.* 2008, 24(18): 10273-10281.

[11]. **Murugesan, S., Xie, J. and Linhardt, R.J.** Immobilization of heparin: approaches and applications. *Current Topics in Medicinal Chemistry.* 2008, 8(2): 80-100.

[12]. **Baveja, J.K., et al.** Furanones as potential anti-bacterial coatings on biomaterials. *Biomaterials.* 2004, 25(20): 5003-5012.

[13]. **Johnson, J.R., et al.** Prevention of catheter-associated urinary tract infection with a silver oxide-coated urinary catheter: clinical and microbiologic correlates. *The Journal of Infectious Diseases.* 1990, 162(5): 1145-1150.

[14]. **DiTizio, V., et al.** A liposomal hydrogel for the prevention of bacterial adhesion to catheters. *Biomaterials.* 1998, 19(20): 1877-1884.

[15]. **Reid, G., et al.** Effects of ciprofloxacin, norfloxacin and ofloxacin on in vitro adhesion and survival of Pseudomonas aeruginosa AK1 on urinary catheters. *Antimicrobial Agents and Chemotherapy.* 1994, 38(7): 1490–1495.

[16]. **Raad, I., et al.** The broad-spectrum activity and efficacy of catheters coated with minocycline and rifampin. *The Journal of Infectious Diseases.* 1996, 173(2): 418-424.

[17]. **Sekiguchi, Y., et al.** Self-sterilizing catheters with titanium dioxide photocatalyst thin films for clean intermittent catheterization: basis and study of clinical use. *International Journal of Urology.* 2007, 14(5): 426-430.

[18]. **Yao, Y., et al.** Self-sterilization using silicone catheters coated with Ag and TiO2 nanocomposite thin film. *Journal of Biomedical Materials Research Part B: Applied Biomaterials.* 2008, 85(2): 453-460.

[19]. **Almeida, E., Diamantino, T.C. and De Sousa, O.** Marine paints: The particular case of antifouling paints. *Progress in Organic Coatings.* 2007, 59(1): 2–20.

[20]. **M., Stanczak.** *Biofouling: It's Not Just Barnacles Anymore.* 2004.

[21]. **Anderson, CA., et al.** The development of foul-release coatings for seagoing vessels. *Journal of Marine Design and Operations.* 2003, B4: 11-23.

[22]. **Schumm, K. and Lam, TBL.** Types of urethral catheters for management of short-term voiding problems in hospitalised adults. *The Cochrane Library.* 2009, CD004013.

[23]. **Beech, IB., et al.** Microbially-influenced corrosion: damage to prostheses, delight for bacteria. *International Journal of Artificial Organs.* 2006, 29(4): 443-452.

[24]. **Hall-Stoodley, L., Costerton, J.W. and Stoodley, P.** Bacterial biofilms: from the natural environment to infectious diseases. *Nature Reviews Microbiology 2.* February 2004, 2: 95-108, pp. 95-108.

[25]. **Lear, G. and Lewis, G.D.** *Microbial Biofilms: Current Research and Applications.* s.l. : Caister Academic Press, 2012. ISBN-10: 1904455964.

[26]. **Parsek, M.R. and Singh, P.K.** Bacterial biofilms: an emerging link to disease pathogenesis. *Annual Reviews in Microbiology.* 2003, 57: 677-701.

[27]. **Licking, E.** Getting a grip on bacterial. *Business week.* 1999, 98-100.

[28]. **Costerton, J.W. et al.** Microbial biofilms. *Annual Review of Microbiology.* 1995, 49: 711–745.

[29]. **Archibald, L.K. and Gaynes, R.P.** Hospital acquired infections in the United States: the importance of interhospital comparisons. *Nosocomial Infect.* 1997, 11: 245–255.

[30]. **Potera, C.** Forging a link between biofilms and disease. *Science.* 1999, 283: 1837–1838.

[31]. **Monroe, D.** Biofilms, Looking for Chinks in the Armor of Bacterial. *PLoS Biology.* 2007, 5 (11): 2458-2461.

[32]. **Löffler, G.** *Basiswissen Biochemie.* Regensburg : Springer Verlag Berlin , 2000. ISBN: 3-540-67389-X.

[33]. **Riva, S.** Laccases: blue enzymes for green chemistry. *Trends in Biotechnology.* 2006, 24(5): 219–226.

[34]. **Claus, H.** Laccases and their occurrence in prokaryotes. *Archives of Microbiology.* 2003, 179: 145–150.

[35]. **Claus, H.** Laccases: structure, reactions, distribution. *Micron.* 2004, 35(1-2): 93–96.

[36]. **Thurston, C.F.** The structure and function of fungal laccases. *Microbiology.* 1994, 140(1): 19–26.

[37]. **Breen A, Singleton FL.** Fungi in lignocellulose breakdown and biopulping. *Current Opinion in Biotechnology.* 1999, 10(3): 252-258.

[38]. **Kawai, S., et al.** Aromatic ring cleavage of 4,6-di(tert-butyl)guaiacol, a phenolic lignin model compound, by laccase of Coriolus versicolor. *FEBS Letters.* 1988, 236(2): 309–311.

[39]. **Duran, N. and Esposito, E.** Potential applications of oxidative enzymes and phenoloxidase-like compounds in wastewater and soil treatment: a review. *Applied Catalysis B: Environmental.* 2000, 28: 83–99.

[40]. **Claus, H., Faber, G. and König, H.** Redox-mediated decolorization of synthetic dyes by fungal laccases. *Applied Microbiology and Biotechnology.* 2002, 59(6): 672-678.

[41]. **Mayer, A.M. and Staples, R.C.** Laccase: new functions for an old enzyme. *Phytochemistry.* 2002, 60(6): 551-65.

[42]. **Kudanga, T., et al.** Potential applications of laccase-mediated coupling and grafting reactions: a review. *Enzyme and Microbial Technology.* 2011, 48: 195-208.

[43]. **Couto, S.R. and Herrera, J.L.T.** Industrial and biotechnological applications of laccases: A review. *Biotechnology Advances.* 2006, 24: 500–513.

[44]. **Upendra, N. D., et al.** Structure–function relationship among bacterial, fungal and plant laccases. *Journal of Molecular Catalysis B: Enzymatic.* 2011, 68 (2): 117–128.

[45]. **Bajpai, P.** Application of enzymes in the pulp and paper industry. *Biotechnology Progress.* 1999, 15(2): 147-157.

[46]. **Rochefort, D., Leech, D. and Bourbonnais, R.** Electron transfer mediator systems for bleaching of paper pulp. *Green Chemistry.* 2004, 6: 14-24.

[47]. **Bourbonnais, R. and Paice, M.G.** Oxidation of non-phenolic substrates. An expanded role for laccase in lignin biodegradation. *FEBS Letters.* 1990, 267(1): 99-102.

[48]. **Reynolds, L.D. and Wilson, N.G.** *Scribes and Scholars 3rd edition.* Oxford : s.n., 1991. 193–194.

[49]. **Vermerris, W. and Nicholson, R.** *Phenolic Compound Biochemistry.* s.l. : Springer Science + Buisness Media B.V., 2008.

[50]. **Kinjo, J., et al.** Activity-Guided Fractionation of Green Tea Extract with Antiproliferative Activity against Human Stomach Cancer Cells. *Biological and Pharmaceutical Bulletin.* 2002, 25(9): 1238—1240.

[51]. **Munoz-Bonilla, A. and Fernandez-Garcıa, M.** Polymeric Materials With Antimicrobial Activity. *Progress in Polymer Science .* 2010.

[52]. **Elvira, G.M., et al.** Catalytic inhibition of human DNA topoisomerase by phenolic compounds in Ardisia compressa extracts and their effect on human colon cancer cells. *Food and chemical Toxicology.* 2006, 44: 1191-1203.

[53]. **Hurrell, R.F., Reddy, M. and Cook, J.D.** Inhibition of non-haem iron absorption in man by polyphenolic-containing beverages. *British Journal of Nutrition.* 1999, 81(4): 289-295.

[54]. **Hsieh, C.L., et al.** Preventive effects of guava (Psidium guajava L.) leaves and its active compounds against alpha-dicarbonyl compounds-induced blood coagulation. *Food Chemistry.* 2007, 103: 528-535.

[55]. **Cook, J.D., Reddy, M.B. and Hurrel, R.F.l.** The effect of red and white wines on nonheme-iron absorption in humans. *The American Journal of Clinical Nutrition.* 1995, 61(4): 800-804.

[56]. **Okabe, N, Kyoyama, H and Suzuki, M.** Gallic acid monohydrate. *Acta Crystallographica Section E.* 2001, 57: 764-766.

[57]. **Masoud, M.S., et al.** Synthesis and spectroscopic characterization of gallic acid and some of its azo complexes. *Journal of Molecular Structure.* 2012, 101(4): 17–25.

58Modification of high-lignin softwood kraft pulp with laccase and amino acids*Enzyme Microb. Technol.*44 (3): 176-181

[59]. **Niedermeyer, T.H.J., Mikolasch, A., Lalk, M.,.** Nuclear amination catalyzed byfungal laccases: reaction products of p-hydroquinones and primary aromatic amines. *J. Org. Chem.* 2005, 70: 2002-2008.

[60]. **Kudanga, T., et al.** Reactivity of long chain alkylamines to lignin moieties: Implications on hydrophobicity of lignocellulose materials. *Journal of Biotechnology.* 2010, 149: 81–87.

[61]. **Pisoschi, A.M., Cheregi, M.C. and A.F., Danet.** Total Antioxidant Capacity of Some Commercial Fruit Juices: Electrochemical and Spectrophotometrical Approaches. *Molecules.* 2009, 14: 480-493.

[62]. **Archambault, J. G. and Brash, J. L.** Protein resistant polyurethane surfaces by chemical grafting of PEO: amino-terminated PEO as grafting reagent. *Colloids Surf B Biointerfaces.* 2004, 39(1-2):9-16.

[63]. **Unsworth, L.D., Sheardown, H. and Brash, J.L.** Protein resistance of surfaces prepared by sorption of end thiolated poly (ethylene glycol) to gold: Effect of surface chain density. *Langmuir.* 2005, 21: 1036-1041.

[64]. **Chang, Y., et al.** Highly protein-resistant coatings from well-defined diblock copolymers containing sulfobetaines. *Langmuir.* 2006, 22(5): 2222-2226.

[65]. **Chang, Y., et al.** Development of biocompatible interpenetrating polymer networks containing a sulfobetaine-based polymer and a segmented polyurethane for protein resistance. *Biomacromolecules.* 2007, 8(1):122-127.

[66]. **Yang, W., et al.** Film thickness dependence of protein adsorption from blood serum and plasma onto poly(sulfobetaine)-grafted surfaces. *Langmuir.* 2008, 24(17): 9211-9214.

[67]. **Kuo, W.H. et al.** Surface Modification with Poly(sulfobetaine methacrylate-co-acrylicacid) To Reduce Fibrinogen Adsorption, Platelet Adhesion and Plasma Coagulation. *Biomacromolecules.* 2011, 12(12): 4348-4356.

[68]. **Griffiths, P. and de Hasseth, J.A.** *Fourier Transform Infrared Spectrometry.* New Jersey : John Wiley & Sons, Inc, 2007. ISBN 978-0-471-19404-2.

[69]. **Brown, R.E., Jarvis, K.L. and Hyland, K.J.** Protein measurement using bicinchoninic acid: elimination of interfering substances. *Analytical Biochemistry.* 1989, 180(1): 136-139.

[70]. **Childs, R.E. and Bardsley, W.G.** The steady-state kinetics of peroxidase with 2,2%-azino-di-(3-ethyl-benzthiazoline-6-sulphonic acid) as chromogen. *Biochemical Journal.* 1975, 145: 93–103.

[71]. **European Committee for Standardization.** *Sterile urethral chatheters for single use.* s.l. : British Standard, 1997. EM1616.

[72]. **Metwalli, E., et al.** Surface characterizations of mono-, di-, and tri-aminosilane treated glass substrates. *Journal of Colloid and Interface Science.* 2006, 298(2): 825-831.

[73]. **Wigfield, D. and Croteau, S.M.** The structure of Ruhemann's purple. *Biochemical Education.* 1980, 8(1): 26-27.

[74]. **Blanco, C.D., et al.** Dyeing properties, synthesis, isolation and characterization of an in situ generated phenolic pigment, covalently bound to cotton. *Enzyme and Microbial Technology.* 2009, 44: 380-385.

[75]. **Korematsu, A., et al.** Synthesis, characterization and platelet adhesion of segmented polyurethanes grafted phospholipid analogous vinyl monomer on surface. *Biomaterials.* 2002, 23: 263–271.

[76]. **Puniredd, S.R., Assad, O. and Haick, H.** Highly Stable Organic Modification of Si(111) Surfaces: Towards Reacting Si with Further Functionalities while Preserving the Desirable Chemical Properties of Full Si-C Atop Site Terminations. *Journal of the American Chemical Society.* 2008, 130; 9184-9185.

[77]. **E.J., Nemanick., et al.** Chemical and electrical passivation of silicon (111) surfaces through functionalization with sterically hindered alkyl groups. *The Journal of Physical Chemistry B.* 2006, 10(30): 14800-14808.

[78]. **Hurley, P.T., et al.** Covalent attachment of acetylene and methylacetylene functionality to Si(111) surfaces: scaffolds for organic surface functionalization while retaining Si-C passivation of Si(111) surface sites. *Journal of the American Chemical Society.* 2006, 128(31): 9990-1.

[79]. **Terry, J., et al.** Determination of the bonding of alkyl monolayers to the Si(111) surface using chemical-shift, scanned-energy photoelectron diffraction . *Applied physics letters.* 1997, 71: 1056-1059.

[80]. **Gao, W., et al.** Protein adsorption and biomimetic mineralization behaviors of PLL–DNA multilayered films assembled onto titanium. *Applied Surface Science.* 2010, 257: 538–546.

[81]. **Borges, A., Saavedra, M.J. and Simões, M.** The activity of ferulic and gallic acids in biofilm prevention and control of pathogenic bacteria. *Biofouling.* 2012, 28(7): 755-67.

[82]. **Stickler, D., et al.** Proteus mirabilis biofilms and the encrustation of urethral catheters. *Urological Research.* 1993, 21: 407-411.